Supporting Information

Design, Synthesis and Operation of Small Molecules that can Walk along Tracks

Max von Delius, Edzard M. Geertsema, David A. Leigh,* Dan-Tam D. Tang

School of Chemistry, University of Edinburgh, The King's Buildings, West Mains Road, Edinburgh EH9 3JJ, UK.

* Fax: +44 131 650 6453; Tel: +44 131 650 4721; E-mail: David.Leigh@ed.ac.uk

Contents

1. Experimental Procedures, Synthesis and Characterization

1.1. General

Unless otherwise stated, all reagents were purchased from commercial sources and used without further purification. Dry CH_2Cl_2, $CHCl_3$ and THF were obtained by passing the solvent through an activated alumina column on a PureSolvTM solvent purification system (InnovativeTechnologies, Inc., MA). Dry DMF and MeOH were purchased from Sigma-Aldrich. Compounds **S1**[2], **S7**[3], **S8-S11**[4] were prepared according to literature procedures. The synthesis of compounds **S6**, **S13**, **S14**, **S18**, **S23**, **S28**, *1,2*-$\mathbf{C_5}$, *3,4*-$\mathbf{C_5}$ and *3,4*-$\mathbf{C_5}$-d_4 has been described previously.[1] Flash column chromatography was carried out using Kieselgel C60 (Merck, Germany) as the stationary phase. Analytical TLC was performed on precoated silica gel plates (0.25 mm thick, 60F254, Merck, Germany) and observed under UV light. All ^{1}H and ^{13}C NMR spectra were recorded on Bruker AV 400, DMX 500, AV 600 or AV 800 (cryoprobe) instruments, at a constant temperature of 298 K. Chemical shifts are reported in parts per million and referenced to residual solvent. Coupling constants (*J*) are reported in Hertz (Hz). Standard abbreviations indicating multiplicity were used as follows: m = multiplet, quint. = quintet, q = quartet, t = triplet, d = doublet, s = singlet, b = broad. Assignment of the ^{1}H NMR signals was accomplished by two-dimensional NMR spectroscopy (COSY, NOESY, HSQC, HMBC). All melting points were determined using a Sanyo Gallenkamp apparatus and are uncorrected. Mass spectrometric analysis was carried out by the mass spectrometry services at the University of Edinburgh and by the EPSRC National Centre at the University of Wales, Swansea. Analytical and preparative HPLC was performed on instruments of Gilson Inc., USA and Agilent Technologies (1200 LC system with photodiode array detector). Normal-phase columns (Kromasil, analytical: 250 × 4.6 mm, semi-preparative: 250 × 10 mm, preparative: 250 × 20 mm) were used with combined isocratic and gradient elution (analytical: 0.8 mL/min, CH_2Cl_2/^{i}PrOH, 3 % → 3 % → 15 % → 15 % → 3 % ^{i}PrOH; semi-preparative: 5 mL/min, CH_2Cl_2/^{i}PrOH, 4.2 % → 4.2 % → 15 % → 15 % → 4.2 % ^{i}PrOH; preparative: 10 mL/min, CH_2Cl_2/MeOH, 1.0 % → 1.0 % → 20 % → 20 % → 1.0 % ^{i}PrOH, UV detection @ 290 nm). LCMS analysis was performed on an Agilent Technologies 1200 LC system with 6130 single quadrupole MS detector (APCI source; positive mode; column and method as specified above).

1.2. Synthetic Schemes

a) Synthesis of walker moieties

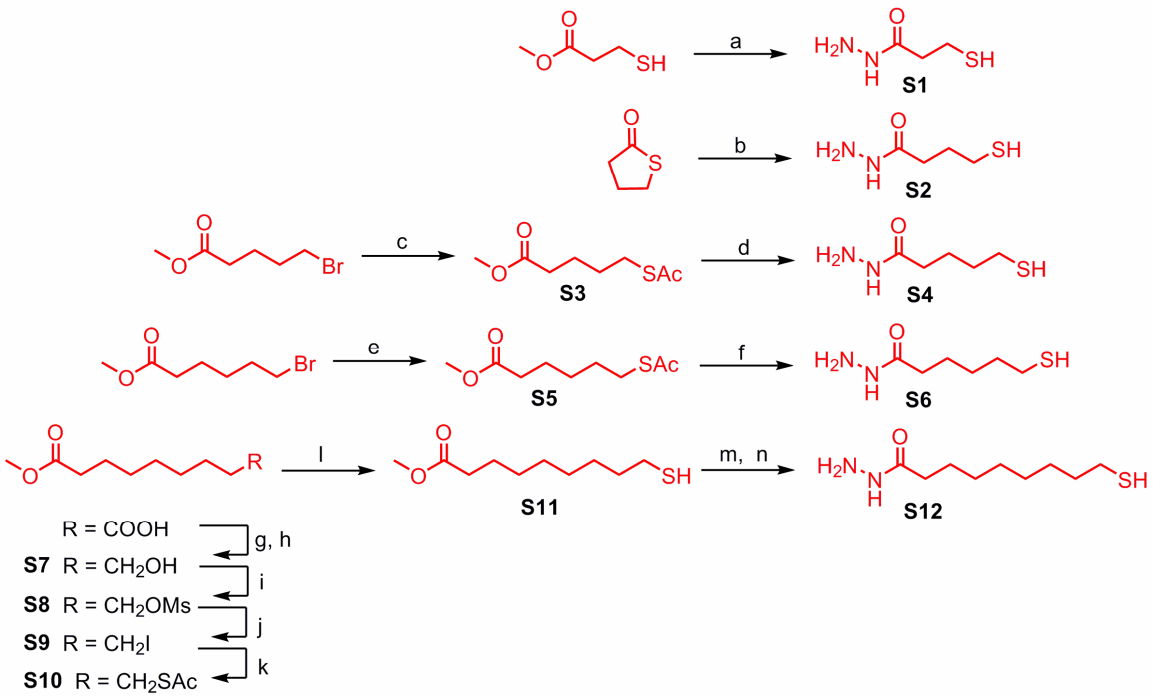

Scheme S1. Reaction conditions: (a) $N_2H_4{\cdot}H_2O$, MeOH, RT, 16 h, 50 %; (b) $N_2H_4{\cdot}H_2O$, MeOH, RT, 30 min, 74 %; (c) KSAc, DMF, RT, 15 min, 98 %; (d) $N_2H_4{\cdot}H_2O$, MeOH, reflux, 16 h, 49 %; (e) KSAc, DMF, RT, 1 h, 85 %; (f) $N_2H_4{\cdot}H_2O$, MeOH, reflux, 16 h, 44 %; (g) $ClCO_2Et$, NEt_3, THF, –5°C, 1 h; (h) $NaBH_4$, H_2O, 0°C, 1 h, 81% (2 steps); (i) NEt_3, CH_2Cl_2, MsCl, 0°C, 1 h, 77%; (j) NaI, acetone, RT, 12 h, 85%; (k) KSAc, DMF, RT, 1 h, 90%; (l) NaOMe, MeOH, RT, 3 h, 79%; (m) $N_2H_4{\cdot}H_2O$, EtOH, reflux, 16 h; (n) DTT, DMF, RT, 16 h, 58 % (two-step).

b) General synthesis of compound series *3,4*-C_n

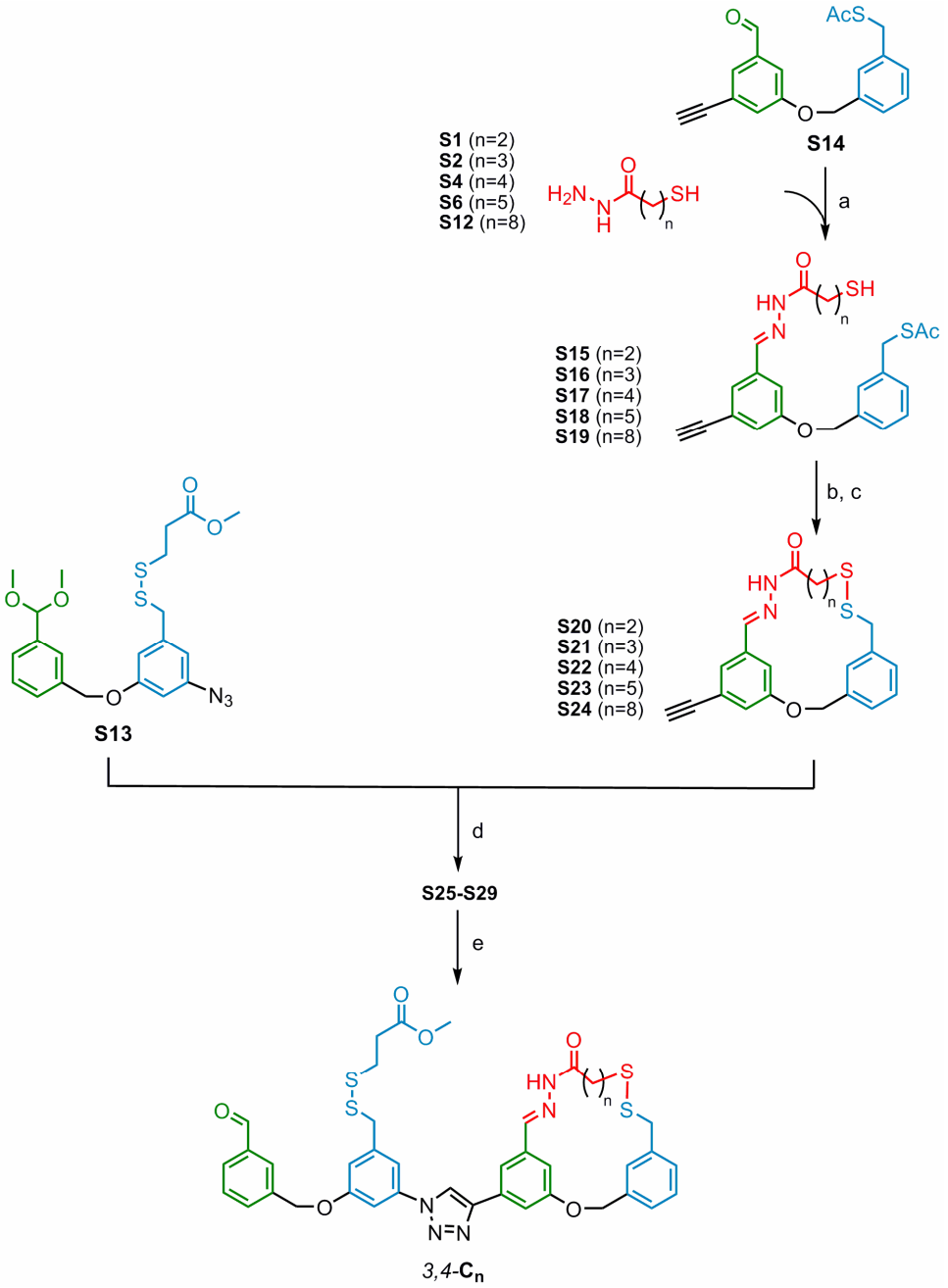

Scheme S2. Reaction conditions: (a) AcOH (cat.), MeOH, RT, 2 h, 73–86 %; (b) NaOMe, MeOH, RT, 2h; (c) I_2, KI, CH_2Cl_2, RT, 5 min, 32–59 % (two-step); (d) $Cu(MeCN)_4PF_6$, tris[(1-benzyl-1*H*-1,2,3-triazol-4-yl)methyl]amine, CH_2Cl_2/THF/MeOH, RT, 16 h, 76–97 %; (e) TFA, CH_2Cl_2, RT, (quant.).

1.3. Synthetic Procedures and Characterization Data

Synthesis of 3-mercaptopropanehydrazide

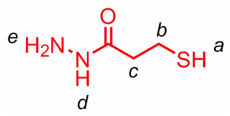

S1

Synthesized according to a modified literature procedure.[2] Under N_2, methyl 3-mercaptopropionate (10 g, 83 mmol, 1.0 equiv.) was added dropwise to a solution of hydrazine monohydrate (10 g, 200 mmol, 2.4 equiv.) in MeOH (30 mL). The reaction mixture was stirred over night at room temperature. Evaporation of the solvent, followed by flash column chromatography (SiO_2, Et_2O/MeOH 8:2) gave **S1** (4.99 g, 50 %) as a colorless oil. ^{1}H NMR (400 MHz, $CDCl_3$): δ = 6.81 (bs, 1H, H_d), 3.93 (bs, 2H, H_e), 2.84 (dt, J = 8.4 Hz, 6.4 Hz, 2H, H_b), 2.50 (t, J = 6.7 Hz, 2H, H_c), 1.61 (t, J = 8.4 Hz, 1H, H_a).

Synthesis of 4-mercaptobutanehydrazide

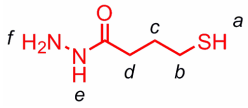

S2

Under N_2, γ-thiobutyrolactone (4.73 g, 46 mmol, 1.0 equiv.) was added dropwise to a solution of hydrazine monohydrate (4.4 g, 68 mmol, 1.5 equiv.) in MeOH (10 mL). The reaction mixture was stirred for 30 min at room temperature. Removal of the solvent under reduced pressure and flash column chromatography (SiO_2, Et_2O/MeOH 5:1) gave **S2** (4.60 g, 74 %) as a colorless oil. ^{1}H NMR (400 MHz, $CDCl_3$): δ = 6.90 (bs, 1H, H_e), 3.90 (bs, 2H, H_f), 2.58 (q, J = 7.2 Hz, 2H, H_b), 2.30 (t, J = 7.3 Hz, 2H, H_d), 1.95 (quint., J = 7.2 Hz, 2H, H_c), 1.33 (t, J = 8.0 Hz, 1H, H_a); ^{13}C NMR (100 MHz, $CDCl_3$): δ = 173.02, 32.48, 29.22, 24.07; HRMS (ESI$^+$): m/z = 135.0588 $[M+H]^+$ (calcd. 135.0587 for $C_4H_{11}ON_2S$).

Synthesis of methyl 5-(acetylthio)pentanoate

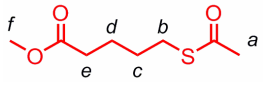

S3

A solution of KSAc (9.02 g, 78.99 mmol, 1.5 equiv.) in DMF (20 mL) was added to a solution of methyl 5-bromopentanoate (9.99 g, 51.20 mmol, 1.0 equiv.) in DMF (30 mL). The reaction was stirred for 15 min at room temperature and the solvent was removed under reduced pressure. The residue was dissolved in Et_2O (50 mL) and saturated NH_4Cl (30 mL) was added. The layers were separated and the aqueous layer was

extracted with Et_2O (4 × 30 mL). The combined organic layers were washed with brine and dried over $MgSO_4$. Removal of the solvent under reduced pressure gave **S3** (9.48 g, 98 %) as a yellowish oil. ^{1}H NMR (400 MHz, $CDCl_3$): δ = 3.68 (s, 3H, H_f), 2.89 (t, J = 7.1 Hz, 2H, H_b), 2.34 (m, 5H, H_a, H_e), 1.66 (m, 4H, H_c, H_d); ^{13}C NMR (100 MHz, $CDCl_3$): δ = 195.84, 173.73, 162.53, 51.58, 36.49, 33.46, 31.43, 30.64, 28.99, 28.63, 23.96; HRMS (ESI$^+$): m/z = 191.0732 $[M+H]^+$ (calcd. 191.0736 for $C_8H_{15}O_3S$).

Synthesis of 5-mercaptopentanehydrazide

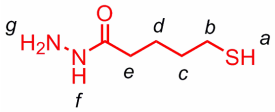

S4

Under N_2, hydrazine monohydrate (8.09 g, 162 mmol, 5 equiv.) was added dropwise to a solution of methyl 5-(acetylthio)pentanoate (4.02 g, 21.13 mmol, 1.0 equiv.) in MeOH (30 mL). The reaction was refluxed over night and the solvent was removed under reduced pressure. Purification by flash column chromatography (SiO_2, Et_2O/MeOH 8:1) gave **S4** (1.51 g, 49 %) as a colorless solid. M.p. 43 °C - 45 °C; ^{1}H NMR (400 MHz, $CDCl_3$): δ = 6.80 (bs, 1H, H_f), 3.92 (bs, 2H, H_g), 2.56 (q, J = 7.3 Hz, 2H H_b), 2.19 (t, J = 7.4 Hz, 2H, H_e), 1.72 (m, 4H, H_c, H_d), 1.39 (t, J = 7.8 Hz, 1H, H_a); ^{13}C NMR (100 MHz, $CDCl_3$): δ = 173.39, 33.84, 33.42, 24.23, 24.11; HRMS (ESI$^+$): m/z = 149.0741 $[M+H]^+$ (calcd. 149.0743 for $C_5H_{13}ON_2S$).

Synthesis of methyl 9-hydroxynonanoate

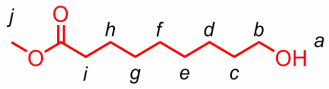

S7

Synthesized according to a literature procedure.[3] ^{1}H NMR (400 MHz, $CDCl_3$): δ = 3.66 (s, 3H, H_j), 3.66 - 3.57 (m, 2H, H_b), 2.30 (t, J = 7.5 Hz, 2H, H_i), 1.68 – 1.49 (m, 4H, $H_{c,h}$), 1.41 – 1.25 (m, 9H, $H_{a,d\text{-}g}$).

Synthesis of methyl 9-mesylnonanoate

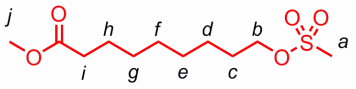

S8

Synthesized according to a literature procedure.[4] ^{1}H NMR (400 MHz, $CDCl_3$): δ = 4.22 (t, J = 6.6 Hz, 2H, H_b), 3.67 (s, 3H, H_j), 3.00 (s, 3H, H_a), 2.30 (t, J = 7.5 Hz, 2H, H_i), 1.78 – 1.71 (m, 2H, H_c), 1.65 – 1.59 (m, 2H, H_h), 1.45 – 1.25 (m, 8H, $H_{d\text{-}g}$).

Synthesis of methyl 9-iodononanoate

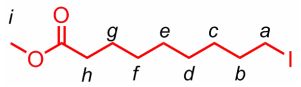

S9

Synthesized according to a literature procedure.[4] ^{1}H NMR (400 MHz, $CDCl_3$): δ = 3.67 (s, 3H, H_i), 3.18 (t, J = 7.0 Hz, 2H, H_a), 2.30 (t, J = 7.5 Hz, 2H, H_h), 1.85 – 1.77 (m, 2H, H_b), 1.65 – 1.58 (m, 2H, H_g), 1.43 - 1.25 (m, 8H, $H_{c\text{-}f}$).

Synthesis of methyl 9-acetylsulfanylnonanoate

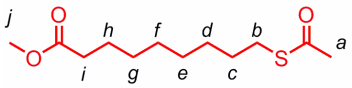

S10

Synthesized according to a literature procedure.[4] ^{1}H NMR (400 MHz, $CDCl_3$): δ = 3.66 (s, 3H, H_j), 2.85 (t, J = 7.3 Hz, 2H, H_b), 2.32 (s, 3H, H_a), 2.30 (t, J = 7.5 Hz, 2H, H_i), 1.64 – 1.51 (m, 4H, $H_{c,h}$), 1.38 – 1.23 (m, 8H, $H_{d\text{-}g}$).

Synthesis of methyl 9-mercaptononanoate

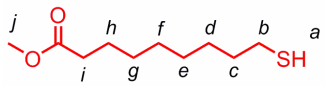

S11

Synthesized according to a literature procedure.[4] ^{1}H NMR (400 MHz, $CDCl_3$): δ = 3.66 (s, 3H, H_j), 2.51 (dt, J = 7.5, 7.2 Hz, 2H, H_b), 2.30 (t, J = 7.5 Hz, 2H, H_i), 1.66 – 1.56 (m, 4H, $H_{c,h}$), 1.41 – 1.27 (m, 9H, $H_{a,d\text{-}g}$).

Synthesis of 9-mercaptononanehydrazide

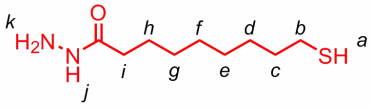

S12

a) **S11** (500 mg, 2.29 mmol) was added dropwise to a solution of hydrazine monohydrate (600 mg, 11.44 mmol) in EtOH (15 mL). This mixture was refluxed over night. Removal of the solvent gave a mixture of product **S12** and the corresponding disulfide, which was used directly for the subsequent reduction step. Characterization data for the disulfide: M.p. 75 °C. ^{1}H NMR (400 MHz, DMSO-d_6): δ = 8.92 (bs, 1H, H_i),

4.08 (bs, 2H, H_j), 2.45 (t, J = 7.1, Hz, 2H, H_a), 1.98 (t, J = 7.4 Hz, 2H, H_h), 1.53 – 1.41 (m, 4H, $H_{b,g}$), 1.35 - 1.17 (m, 8H, H_{c-f}).

b) The crude mixture of disulfide and thiol **S12** was dissolved in dry DMF (10 mL) and dithiothreitol (160 mg, 1.03 mmol, 1.1 equiv.) was added. The mixture was stirred at room temperature over night and the bulk of the solvent was removed under reduced pressure. Flash column chromatography (SiO_2, Et_2O/MeOH 9:1) gave **S12** (254 mg, 58 % two-step yield) as a colorless solid. M.p. 70 °C. ^{1}H NMR (400 MHz, $CDCl_3$): δ = 6.65 (bs, 1H, H_j), 3.89 (bs, 2H, H_k), 2.52 (q, J = 7.4 Hz, 2H H_b), 2.14 (t, J = 7.6 Hz, 2H, H_i), 1.67-1.56 (m, 4H, H_c, H_h), 1.40-1.27 (m, 5H, H_a, H_g, H_f, H_e, H_d); ^{13}C NMR (100 MHz, $CDCl_3$): δ = 173.91, 34.51, 33.92, 29.14, 29.12, 28.83, 28.23, 25.40, 24.59; HRMS (ESI^+): m/z = 205.1372 $[M+H]^+$ (calcd. 205.1369 for $C_9H_{21}ON_2S$).

General synthetic procedure for compounds S15-S19

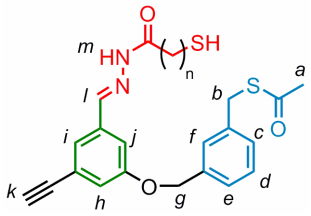

S15 (n=2), **S16** (n=3), **S17** (n=4), **S18** (n=5),[1] **S19** (n=8)

Under N_2, **S14** (900 mg, 2.76 mmol, 1.0 equiv.) was dissolved in dry MeOH (c ≈ 0.1 M). After addition of 3-5 drops of acetic acid, a solution of the walker hydrazide (**S1**/**S2**/**S4**/**S6**/**S12**) (1.1-1.7 equiv.) in dry MeOH (c ≈ 0.5 M) was added dropwise. The reaction was monitored by TLC (SiO_2, *n*-hexane/EtOAc 3:2). After 2 h the reaction was usually complete and the solvent was removed under reduced pressure. Purification by flash column chromatography (SiO_2, *n*-hexane/EtOAc 3:2) gave the pure compounds.

S15 (n=2): (*E*)-*S*-3-((3-ethynyl-5-((2-(3-mercaptopropanoyl)hydrazono)methyl)phenoxy)methyl)benzyl ethanethioate. **S14** (900 mg, 2.76 mmol, 1.0 equiv.) and **S1** (500 mg, 4.76 mmol, 1.7 equiv.) gave **S15** (954 mg, 81%) as a colorless solid. ^{1}H NMR (400 MHz, $CDCl_3$): δ = 8.92 (s, 1H, H_m), 7.64 (s, 1H, H_l), 7.36–7.26 (m, 6H, H_{Ar}), 7.12 (dd, J = 2.4 Hz, 1.3 Hz, 1H, H_{Ar}), 5.06 (s, 2H, H_g), 4.14 (s, 2H, H_b), 3.10 (t, J = 6.8 Hz, 2H, H_n), 3.10 (s, 1H, H_k), 2.90 (dt, J = 8.3 Hz, 6.8 Hz, 2H, H_o), 2.36 (s, 3H, H_a), 1.74 (t, J = 8.3 Hz, 1H, H_p); ^{13}C NMR (100 MHz, $CDCl_3$); δ = 195.09, 173.49, 158.74, 142.42, 138.25, 136.64, 135.12, 129.05, 128.76, 127.97, 126.50, 124.03, 123.76, 119.74, 113.95, 82.71, 77.93, 70.06, 36.90, 33.28, 30.38, 19.35; HRMS (ESI^+): m/z = 427.1145 $[M+H]^+$ (calcd. 427.1145 for $C_{22}H_{23}N_2O_3S_2$).

S16 (n=3): (*E*)-*S*-3-((3-ethynyl-5-((2-(4-mercaptobutanoyl)hydrazono)methyl)phenoxy)methyl)benzyl ethanethioate. **S14** (164 mg, 0.51 mmol, 1.0 equiv.) and **S2** (75 mg, 0.56 mmol, 1.1 equiv.) gave **S16** (180 mg, 81%) as a yellowish powder. M.p. 110 °C; ^{1}H NMR (400 MHz, $CDCl_3$): δ = 8.74 (s, 1 H, H_m), 7.62 (s, 1 H, H_l), 7.37-7.27 (m, 6 H, H_{Ar}), 7.12 (dd, J = 2.31 Hz, 1.27 Hz, 1 H, H_{Ar}), 5.06 (s, 2 H, H_g), 4.14 (s, 2 H, H_b), 3.11 (s, 1 H, H_k), 2.89 (t, J = 7.3 Hz, 2 H, H_n), 2.67 (dt, J = 7.4 Hz, 2 H, H_p), 2.36 (s, 3 H, H_a), 2.05 (tt,

J = 7.1 Hz, 2 H, H_o), 1.74 (m, 2 H, H_p), 1.39 (t, J = 8.1 Hz, 1 H, H_q); ^{13}C NMR (100 MHz, $CDCl_3$): δ = 195.05, 174.90, 158.75, 141.96, 138.25, 136.65, 135.22, 129.04, 128.75, 127.97, 126.49 (2 C), 124.03, 123.74, 119.70, 113.86, 82.73, 70.05, 33.28, 31.15, 30.37, 28.74, 24.30; HRMS (ESI$^+$): m/z = 441.1300 $[M+H]^+$ (calcd. 441.1301 for $C_{23}H_{25}N_2O_3S_2$).

S17 (n=4): (*E*)-*S*-3-((3-ethynyl-5-((2-(5-mercaptopentanoyl)hydrazono)methyl)phenoxy)methyl)benzyl ethanethioate. **S14** (140 mg, 0.43 mmol, 1.0 equiv.) and **S4** (70 mg, 0.48 mmol, 1.1 equiv.) gave **S17** (143 mg, 73%) as a yellowish powder. M.p. 109 °C; ^{1}H NMR (400 MHz, $CDCl_3$): δ = 8.80 (s, 1 H, H_m), 7.63 (s, 1 H, H_l), 7.39-7.27 (m, 6 H, H_{Ar}), 7.12 (dd, J = 2.3 Hz, 1.2 Hz, 1 H, H_{Ar}), 5.06 (s, 2 H, H_g), 4.14 (s, 2 H, H_b), 3.11 (s, 1 H, H_k), 2.77 (t, J = 7.3 Hz, 2 H, H_n), 2.60 (dt, J = 7.3 Hz, 2 H, H_q), 2.36 (s, 3 H, H_a), 1.84 (m, 2 H, H_o), 1.74 (m, 2 H, H_p), 1.39 (t, J = 7.9 Hz, 1 H, H_r); ^{13}C NMR (100 MHz, $CDCl_3$): δ = 195.05, 175.51, 158.75, 141.95, 138.25, 136.65, 135.31, 129.04, 128.76, 127.98, 126.51 (2 C), 123.97, 123.72, 119.56, 113.95, 82.76, 70.05, 33.61, 33.28, 32.05, 30.37, 24.39, 23.26; HRMS (ESI$^+$): m/z = 455.1459 $[M+H]^+$ (calcd. 455.1458 for $C_{24}H_{27}N_2O_3S_2$).

S19 (n=8): (*E*)-*S*-3-((3-ethynyl-5-((2-(9-mercaptononanoyl)hydrazono)methyl)phenoxy)methyl)benzyl ethanethioate. **S14** (256 mg, 0.79 mmol, 1.0 equiv.) and **S12** (243 mg, 1.19 mmol, 1.5 equiv.) gave **S19** (343 mg, 85%) as a colorless, waxy solid. M.p. 93 °C. ^{1}H NMR (400 MHz, $CDCl_3$): δ = 8.78 (s, 1H, H_m), 7.62 (s, 1H, H_l), 7.36 – 7.28 (m, 6H, H_{Ar}), 7.11 (s, J = 2.3 Hz, 1.3 Hz, 1H, H_{Ar}), 5.05 (s, 2H, H_g), 4.16 (s, 2H, H_b), 3.11 (s, 1H, H_k), 2.74 (t, J = 7.6 Hz, 2H, H_n), 2.50 (q, J = 7.4 Hz, 2H, H_u), 2.36 (s, 3H, H_a), 1.72 (quint., J = 7.4 Hz, 2H, H_o), 1.59 (quint., J = 7.2 Hz, 2H, H_t), 1.37 (m, 8H, H_s, H_r, H_q, H_p), 1.31 (t, J = 7.7 Hz, 1H, H_v); ^{13}C NMR (100 MHz, $CDCl_3$): δ = 195.02, 176.11, 158.70, 141.70, 138.22, 136.62, 135.39, 129.01, 128.74, 127.98, 126.50, 126.43, 123.86, 123.66, 119.41, 114.01, 82.78, 70.02, 34.00, 33.25 (2C), 32.60, 30.33, 29.24, 28.90, 28.30, 24.61 (2C); HRMS (ESI$^+$): m/z = 511.2084 $[M+H]^+$ (calcd. 511.2084 for $C_{28}H_{35}N_2O_3S_2$).

General synthetic procedure for compounds S20-S24

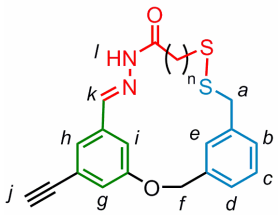

S20 (n=2), **S21** (n=3), **S22** (n=4), **S23** (n=5),[1] **S24** (n=8)

Under N_2, thioacetate (**S15-19**) (1.0 equiv.) was dissolved in a 1:1 mixture of MeOH and CH_2Cl_2 (c ≈ 0.05 M). A solution of NaOMe (1.5 - 2.0 equiv.) in MeOH (c ≈ 0.5 M) was added. After 2 h of stirring at room temperature, the mixture was diluted with CH_2Cl_2 (c ≈ 0.005 M) and KI (0.2 equiv.) was added. A solution of I_2 (1.0 equiv.) in CH_2Cl_2 (c ≈ 0.1 M) was added dropwise until the brown color persisted. Na_2SO_3 was added to reduce the excess of I_2 and, when decolorization was complete, stirring was continued for 15

min. H_2O was added and the phases were separated. The H_2O layer was extracted another time with CH_2Cl_2. The combined organic layers were washed with brine and dried ($MgSO_4$). Removal of the solvents under reduced pressure and purification by flash column chromatography (SiO_2, CH_2Cl_2/EtOAc 9:1) gave the pure compounds.

S20 (n=2): (*E*)-20-Ethynyl-2-oxa-10,11-dithia-15,16-diaza-tricyclo[16.3.1.1^{4,8}]tricosa-1(21),4(23),5,7,16,18(22),19-heptaen-14-one. **S15** (570 mg, 1.34 mmol, 1.0 equiv.) gave **S20** (300 mg, 59%) as a colorless solid. ^{1}H NMR (400 MHz, DMSO-d$_6$): δ = 11.66 (s, 1H, H$_l$), 8.07 (s, 1H, H$_k$), 7.83 (s, 1H, H$_{Ar}$), 7.70 (s, 1H, H$_{Ar}$), 7.55–7.43 (m, 3H, H$_{Ar}$), 7.32 (d, *J* = 2.4 Hz, 1H, H$_{Ar}$), 7.30 (s, 1H, H$_{Ar}$), 5.54 (s, 2H, H$_f$), 4.48 (s, 1H, H$_j$), 4.19 (s, 2H, H$_a$), 3.39 (dd, *J* = 6.8 Hz, 6.5 Hz, 2H, H$_m$ or H$_l$), 3.24 (dd, *J* = 6.8 Hz, 6.5 Hz, 2H, H$_m$ or H$_l$); ^{13}C NMR (100 MHz, DMSO-d$_6$); δ = 172.44, 157.79, 141.06, 137.12, 136.97, 136.01, 129.68, 129.07, 128.28, 126.06, 125.34, 123.25, 122.40, 108.37, 82.40, 79.14, 69.02, 41.04, 31.14, 30.31; HRMS (ESI$^+$): *m*/*z* = 383.0881 [M+H]$^+$ (calcd. 383.0882 for $C_{20}H_{19}N_2O_2S_2$).

S21 (n=3): (*E*)-21-Ethynyl-2-oxa-10,11-dithia-16,17-diaza-tricyclo[17.3.1.1^{4,8}]tetracosa-1(23),4,6,8(24),17,19,21-heptaen-15-one. **S16** (178 mg, 0.40 mmol, 1.0 equiv.) gave **S21** (71 mg, 44%) as a colorless solid. M.p. 210 °C; ^{1}H NMR (400 MHz, $CDCl_3$): δ = 9.40 (s, 1H, H$_l$), 7.61 (s, 1H, H$_k$), 7.36-7.28 (m, 4H, H$_{Ar}$), 7.28-7.25 (m, 1H, H$_{Ar}$) 7.23 (m, 1H, H$_{Ar}$), 7.04 (s, 1H, H$_{Ar}$), 5.30 (s, 2H, H$_f$), 3.86 (s, 2H, H$_a$), 3.10 (s, 1H, H$_j$) 2.69 (t, *J* = 7.4 Hz, 2H, H$_o$), 2.31 (t, *J* = 7.4 Hz, 2H, H$_m$), 1.97 (quint., *J* = 7.4 Hz, 2H, H$_n$); ^{13}C NMR (100 MHz, $CDCl_3$): *δ* = 175.07, 159.07, 141.81, 138.51, 137.72, 135.21, 128.94, 128.35, 126.28, 126.23, 124.70, 123.94, 123.70, 108.83, 82.35, 70.43, 43.27, 38.32, 32.03, 25.34; HRMS (EI$^+$): *m*/*z* = 396.0962 [M]$^+$ (calcd. 396.0961 for $C_{21}H_{20}N_2O_2S_2$).

S22 (n=4): (*E*)-22-Ethynyl-2-oxa-10,11-dithia-17,18-diaza-tricyclo[19.3.1.1^{4,8}]pentacosa-1(24),4,6,8(25),18,20,22-heptaen-16-one. **S17** (135 mg, 0.30 mmol, 1.0 equiv.) gave **S22** (57 mg, 47 %) as a colorless solid. M.p. 210 °C; ^{1}H NMR (400 MHz, $CDCl_3$): δ = 9.54 (s, 1H, H$_l$), 7.65 (s, 1H, H$_k$), 7.36 (m, 1H, H$_{Ar}$), 7.33 (bs, 1H, H$_{Ar}$), 7.29-7.23 (m, 3H, H$_{Ar}$), 7.15 (d, 1H, H$_{Ar}$), 7.07 (bs, 1H, H$_{Ar}$), 5.33 (s, 2H, H$_f$), 3.86 (s, 2H, H$_a$), 3.11 (s, 1H, H$_j$), 2.56 (m, 2H, H$_p$), 2.26 (m, 2H, H$_m$), 1.68 (m, 2H, H$_n$), 1.59 (m, 2H, H$_o$); ^{13}C NMR (100 MHz, $CDCl_3$): δ = 175.74, 159.11, 141.83, 138.63, 137.42, 135.30, 128.85 (2C), 128.20, 126.54, 126.44, 124.45, 123.84, 123.41, 108.90, 82.35, 69.85, 44.01, 37.84, 32.47, 29.06, 24.38; HRMS (EI$^+$): *m*/*z* = 410.1116 [M]$^+$ (calcd. 410.1117 for $C_{22}H_{22}N_2O_2S_2$).

S24 (n=8): (*E*)-26-Ethynyl-2-oxa-10,11-dithia-21,22-diaza-tricyclo[22.3.1.1^{4,8}]nonacosa-1(27),4(29),5,7,22,24(28),25-heptaen-20-one. **S19** (316 mg, 0.62 mmol, 1.0 equiv.) gave **S24** (95 mg, 32 %) as a colorless solid. ^{1}H NMR (400 MHz, $CDCl_3$): δ = 8.64 (s, 1H, H$_l$), 7.65 (s, 1H, H$_k$), 7.55 (s, 1H, H$_{Ar}$), 7.43 (s, 1H, H$_{Ar}$), 7.39-7.33 (m, 3H, H$_{Ar}$), 7.17 (m, 1H, H$_{Ar}$), 7.12 (s, 1H, H$_{Ar}$), 5.03 (s, 2H, H$_f$), 3.68 (s, 2H, H$_a$), 3.11 (s, 1H, H$_j$), 2.72 (m, 2H, H$_m$), 2.06 (t, *J* = 7.1 Hz, 2H, H$_t$), 1.77 (m, 2H, H$_n$), 1.40-12.21 (m, 10H, H$_s$, H$_r$, H$_q$, H$_p$, H$_o$); ^{13}C NMR (100 MHz, $CDCl_3$): δ = 176.78, 158.86, 141.63, 138.51, 135.89, 135.53, 129.61, 129.56, 128.97, 127.29, 125.99, 123.72, 120.77, 109.92, 82.56, 70.10, 43.01, 38.96, 33.00, 30.29, 29.31, 29.25, 28.71, 28.66, 28.58, 25.32; HRMS (ESI$^+$): *m*/*z* = 467.1821 [M+H]$^+$ (calcd. 467.1821 for $C_{26}H_{31}N_2O_2S_2$).

General synthetic procedure for compounds S25-S29

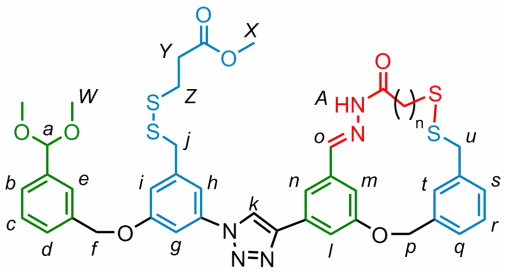

S25 (n=2), **S26** (n=3), **S27** (n=4), **S28** (n=5),[1] **S29** (n=8)

Under N_2, **S13** (1.0 equiv.) was dissolved in DCM (c ≈ 0.02 M) and a solution of the alkyne (**S20**-**S25**) (1.0-1.2 equiv.) in THF (c ≈ 0.02 M) was added. Tris[(1-benzyl-1*H*-1,2,3-triazol-4-yl)methyl]amine (0.1 equiv.) and $Cu(MeCN)_4PF_6$ (0.1 equiv.) were dissolved in MeOH (c ≈ 0.01 M) and the solution was added to the reaction mixture, which was allowed to stir over night at room temperature. Removal of the solvents under reduced pressure followed by flash column chromatography (SiO_2, DCM/EtOAc 85:15 → 7:3) gave the pure compounds.

S25 (n=2): **S13** (37 mg, 80 µmol, 1.0 equiv.) and **S20** (31 mg, 80 µmol, 1.0 equiv.) gave **S25** (61 mg, 90 %) as a colorless solid. M.p. 142 °C. ^{1}H NMR (400 MHz, $CDCl_3$): δ = 9.45 (s, 1H, H_A), 8.25 (s, 1H, H_k), 7.74 (s, 1H, H_o), 7.57 (m, 2H, H_e, H_l), 7.52 (s, 1H, H_n), 7.49 (s, 1H, H_t), 7.42 (m, 5H, H_b, H_c, H_d, H_g, H_q), 7.34 (s, 1H, H_h), 7.30 (m, 2H, H_r, H_m), 7.20 (d, *J* = 7.3 Hz, H_s), 7.03 (s, 1H, H_i), 5.43 (s, 1H, H_a), 5.32 (s, 2H, H_p), 5.17 (s, 2H, H_f), 3.92 (s, 2H, H_u or H_j), 3.90 (s, 2H, H_u or H_j), 3.67 (s, 3H, H_X), 3.35 (s, 6H, H_W), 3.17 (t, *J* = 7.4 Hz, 2H, H_B), 2.95 (t, *J* = 7.4 Hz, 2H, H_C), 2.77 (m, 2H, H_Z), 2.67 (m, 2H, H_Y); ^{13}C NMR (100 MHz, $CDCl_3$): δ = 173.26, 172.15, 159.78, 159.01, 147.27, 142.87, 140.77, 138.70, 137.90, 137.63, 137.40, 136.11, 135.32, 132.00, 129.34, 128.68, 128.39, 128.25, 127.66, 126.74, 126.19, 125.91, 120.32, 118.10, 117.62, 116.18, 113.44, 108.48, 106.37, 102.88, 70.41, 70.23, 52.82, 51.96, 43.38, 43.03, 33.88, 33.03, 32.46, 32.12; HRMS (ESI^+): *m*/*z* = 800.1705 $[M\text{-acetal+H}]^+$ (calcd. 800.1699 for $C_{39}H_{38}N_5O_6S_4$).

S26 (n=3): **S13** (29 mg, 63 µmol, 1.0 equiv.) and **S21** (30 mg, 76 µmol, 1.2 equiv.) gave **S26** (41 mg, 76 %) as a colorless solid. M.p. 138 °C; ^{1}H NMR (400 MHz, $CDCl_3$): δ = 9.84 (s, 1H, H_A), 8.28 (s, 1H, H_k), 7.82 (s, 1H, H_o),7.61-7.60 (m, 1H, H_l), 7.57 (bs, 1H, H_b), 7.54 (bs, 1H, H_n), 7.46-7.38 (m, 4H, H_g, H_c, H_d, H_e), 7.37 (bs, 1H, H_t), 7.35 (bs, 1H, H_h), 7.33-7.26 (m, 4H, H_q, H_r, H_s, H_m), 7.03 (bs, 1H, H_i), 5.43 (s, 1H, H_a), 5.34 (s, 2H, H_p), 5.17 (s, 2H, H_f), 3.92 (s, 2H, H_j), 3.86 (s, 2H, H_u), 3.67 (s, 3H, H_X), 3.35 (s, 6H, H_W), 2.77 (t, *J* = 6.7 Hz, 2H, H_Y or H_Z), 2.69 (m, 4H, H_B, H_Y or H_Z), 2.32 (t, *J* = 7.4 Hz, 2H, H_D), 1.98 (t, *J* = 7.4 Hz, 2H, H_C); ^{13}C NMR (100 MHz, $CDCl_3$): δ = 175.46, 172.15, 159.77, 159.75, 147.29, 142.86, 140.78, 138.69, 138.49, 138.02, 137.90, 136.13, 135.93, 131.94, 128.89, 128.67, 128.31, 127.67, 126.72, 126.29, 125.91, 124.73, 120.53, 118.16, 117.37, 116.19, 113.43, 108.01, 106.28, 102.89, 70.47, 70.39, 52.82, 51.96, 43.30,

43.02, 38.37, 33.87, 33.02, 32.14, 25.52; HRMS (ESI$^+$): m/z = 877.2539 $[M+NH_4]^+$ (calcd. 877.2540 for $C_{42}H_{49}N_6O_7S_4$).

S27 (n=4): **S13** (28 mg, 61 µmol, 1.0 equiv.) and **S22** (30 mg, 73 µmol, 1.2 equiv.) gave **S27** (43 mg, 80 %) as a colorless solid. M.p. 210 °C; ^{1}H NMR (400 MHz, $CDCl_3$): δ = 9.87 (s, 1H, H_A), 8.29 (s, 1H, H_k), 7.84 (s, 1H, H_a), 7.63-7.62 (m, 1 H, H_l), 7.57 (s, 2H, H_b, H_n), 7.45-7.41 (m, 4H, H_g, H_c, H_d, H_e), 7.36-7.33 (m, 3H, H_h, H_m, H_t), 7.28-7.26 (m, 2H, H_r, H_s), 7.26-7.20 (m, 1 H, H_q), 7.04 (bs, 1H, H_i), 5.43 (s,1H, H_o),5.39 (s, 2H, H_p), 5.17 (s, 2H, H_f), 3.92 (s, 2H, H_j), 3.86 (s, 2H, H_u), 3.67 (s, 3H, H_X), 3.35 (s, 6H, H_W), 2.77 (t, J = 6.6 Hz, 2H, H_Y or H_Z), 2.67 (t, J = 6.7 Hz, 2H, H_Y or H_Z), 2.58 (m, 2H, H_B), 2.27 (m, 2H, H_E), 1.70 (t, J = 7.3 Hz, 2H, H_C), 1.59 (t, J = 7.2 Hz, 2H, H_D); ^{13}C NMR (100 MHz, $CDCl_3$): δ = 176.05, 172.14, 159.78 (2C), 147.27, 142.84, 140.79, 138.70, 138.59, 137.90, 137.69, 136.12, 135.96, 132.09, 128.84, 128.67, 128.13, 127.66, 126.73, 126.45, 125.91, 124.50, 120.75, 118.20, 116.90, 116.20, 113.43, 107.96, 106.30, 102.88, 70.40, 69.83, 52.82, 51.96, 44.02, 43.02, 37.86, 33.87, 33.02, 32.55, 29.12, 24.50; HRMS (ESI$^+$): m/z = 891.2696 $[M+NH_4]^+$ (calcd. 891.2697 for $C_{43}H_{51}N_6O_7S_4$).

S29 (n=8): **S13** (48 mg, 103 µmol, 1.0 equiv.) and **S24** (58 mg, 124 µmol, 1.2 equiv.) gave **S25** (91 mg, 97 %) as a colorless solid. ^{1}H NMR (400 MHz, $CDCl_3$): δ = 8.99 (s, 1H, H_A), 8.26 (s, 1H, H_k), 7.81 (s, 1H, H_o), 7.62-7.54 (m, 4H, H_c, H_l, H_n, H_t), 7.47-7.32 (m, 9H, H_b, H_d, H_e, H_g, H_h, H_m, H_q, H_r, H_s), 7.04 (bs, 1H, H_i), 5.43 (s, 1H, H_a), 5.17 (s, 2H, H_p), 5.13 (s, 2H, H_f), 3.92 (s, 2H, H_j), 3.87 (s, 2H, H_u), 3.66 (s, 3H, H_X), 3.34 (s, 6H, H_W), 2.80-2.72 (m, 4H, H_B, H_Y or H_Z), 2.67 (t, J = 7.7 Hz ,2H, H_Y or H_Z), 2.07 (t, J = 7.0 Hz, 2H, H_I), 1.85-1.75 (m, 2H, H_C), 1.52-1.34 (m, 6H, H_D, H_G, H_H), 1.34-1.16 (m, 4H, H_E, H_F). ^{13}C NMR (100 MHz, $CDCl_3$): δ = 176.76, 172.09, 159.75, 159.59, 147.38, 142.29, 140.75, 138.67, 138.45, 137.87, 136.12, 136.07, 136.06, 132.02, 129.58, 129.53, 128.96, 128.62, 127.61, 127.29, 126.69, 125.86, 120.08, 118.12, 116.16, 114.60, 113.40, 108.80, 106.32, 102.85, 70.37, 70.14, 52.77, 51.90, 43.01 (2C), 38.97, 33.84, 33.07, 33.00, 29.39, 29.33, 28.77, 28.68, 28.63, 25.37; HRMS (ESI$^+$): m/z = 947.3323 $[M+NH_4]^+$ (calcd. 947.3328 for $C_{47}H_{59}N_6O_7S_4$).

Note: Assignment of the ^{1}H NMR signals was accomplished by means of 2-D NMR (COSY, ROESY, HMQC, HMBC).

General synthetic procedure for compounds *3,4*-C_n

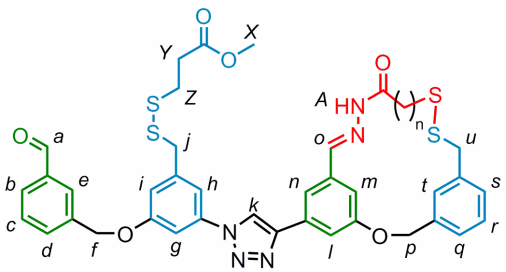

***3,4*-C_n**

The acetal (**S25**-**S29**) (1.0 equiv.) was dissolved in $CHCl_3$ (c ≈ 0.01 M) and 3 drops of TFA were added. The solution was vigorously stirred for 1 minute before saturated $NaHCO_3$ was added. The layers were separated and the aqueous phase was extracted with $CHCl_3$. The combined organic layers were dried over $MgSO_4$. The pure compounds were obtained as colorless solids in quantitative yield (HPLC). This deprotection procedure was carried out in small batches (1-5 mg of starting material) and the obtained product was used directly for subsequent experiments.

3,4-**C**$_3$: ^{1}H NMR (400 MHz, $CDCl_3$): δ = 10.07 (s, 1H, H_a), 9.00 (s, 1H, H_A), 8.29 (s, 1H, H_k), 8.02 (s, 1H, H_e), 7.88 (d, *J* = 7.6 Hz, 1H, H_b), 7.76-7.73 (m, 2H, H_o, H_d), 7.63-7.59 (m, 2H, H_c, H_l), 7.56 (s, 1H, H_n), 7.46 (t, *J* = 2.0 Hz, 1H, H_g), 7.38-7.28 (m, 6H, H_h, H_m, H_q, H_r, H_s, H_t), 7.05 (bs, 1H, H_i), 5.35 (s, 2H, H_p), 5.26 (s, 2H, H_f), 3.94 (s, 2H, H_j), 3.87 (s, 2H, H_u), 3.68 (s, 3H, H_X), 2.78 (t, *J* = 6.7 Hz, 2H, H_Y or H_Z), 2.73 (t, *J* = 7.4 Hz, 2H, H_B), 2.68 (t, *J* = 6.7 Hz, 2H, H_Y or H_Z), 2.35 (t, *J* = 7.4 Hz, 2H, H_D), 2.00 (quint., *J* = 7.4 Hz, 2H, H_C); ^{13}C NMR (100 MHz, $CDCl_3$): δ = 190.99, 174.41, 173.86, 158.72, 158.43, 146.30, 141.29, 139.93, 137.46, 136.94, 136.90, 136.30, 135.74, 134.72, 132.26, 130.89, 128.82, 128.47, 127.91, 127.29, 127.24, 125.29, 123.73, 119.39, 117.07, 116.44, 115.08, 112.62, 107.03, 105.24, 69.43, 68.57, 50.95, 42.25, 41.91, 37.33, 32.84, 32.00, 31.04, 24.33; HRMS (ESI^+): *m*/*z* = 814.1847 $[M+H]^+$ (calcd. 814.1856 for $C_{40}H_{40}N_5O_6S_4$).

3,4-**C**$_4$: ^{1}H-NMR (400 MHz, $CDCl_3$): δ = 10.07 (s, 1H, H_a), 8.96 (s, 1H, H_A), 8.30 (s, 1H, H_k), 8.02 (s, 1H, H_e), 7.88 (d, *J* = 7.6 Hz, 1H, H_b), 7.76-7.74 (m, 2H, H_o, H_d), 7.63-7.54 (m, 2H, H_c, H_l), 7.52 (s, 1H, H_n), 7.46 (t, *J* = 2.0 Hz, 1H, H_g), 7.38-7.37 (m, 3H, H_h, H_m, H_t), 7.29-7.26 (m, 2H, H_r, H_q), 7.22-7.20 (m, 1H, H_s), 7.06 (bs, 1H, H_i), 5.40 (s, 2H, H_p), 5.26 (s, 2H, H_f), 3.94 (s, 2H, H_j), 3.87 (s, 2H, H_u), 3.67 (s, 3H, H_X), 2.78 (t, *J* = 6.7 Hz, 2H, H_Y or H_Z), 2.68 (t, *J* = 6.7 Hz, 2H, H_Y or H_Z), 2.59 (m, 2H, H_B), 2.28 (m, 2H, H_E), 1.70 (quint, *J* = 7.2 Hz, 2H, H_C), 1.60 (quint, *J* = 7.3 Hz, 2H, H_D). ^{13}C NMR (100 MHz, $CDCl_3$): δ = 192.01, 175.42, 172.13, 159.82, 159.48, 147.32, 142.27, 140.99, 138.63, 137.98, 137.64, 137.34, 136.78, 135.79, 133.29, 132.08, 129.88, 129.50, 128.86, 128.24, 128.16, 126.43, 124.49, 120.65, 118.14, 117.03, 116.13, 113.66, 108.02, 106.31, 69.85, 69.62, 51.97, 44.04, 42.96, 37.87, 33.88, 33.05, 32.54, 29.09, 24.38; HRMS (ESI^+): *m*/*z* = 828.2005 $[M+H]^+$ (calcd. 828.2012 for $C_{41}H_{42}N_5O_6S_4$).

3,4-**C**$_8$: ^{1}H NMR (400 MHz, $CDCl_3$): δ = 10.07 (s, 1H, H_a), 8.90 (s, 1H, H_A), 8.28 (s, 1H, H_k), 8.01 (s, 1H, H_e), 7.88 (d, *J* = 7. Hz, 1H, H_b), 7.80 (bs, 1H, H_o), 7.74 (d, *J* = 7.6 Hz, 1H, H_d), 7.62-7.55 (m, 4H, H_c, H_g, H_l, H_n), 7.38-7.37 (m, 6H, H_h, H_m, H_q, H_r, H_s, H_t), 7.05 (bs, 1H, H_i), 5.25 (s, 2H, H_p), 5.13 (s, 2H, H_f), 3.93 (s, 2H, H_j), 3.66 (s, 3H, H_X), 2.79-2.71 (m, 4H, H_B, H_Y or H_Z), 2.67 (t, *J* = 6.8 Hz, 2H, H_Y or H_Z), 2.07 (t, *J* = 7.0 Hz, 2H, H_l), 1.85-1.77 (m, 2H, H_C), 1.48-1.36 (m, 6H, H_D, H_G, H_H), 1.35-1.25 (m, 4H, H_E, H_F); ^{13}C NMR (100 MHz, $CDCl_3$): δ = 192.00, 176.22, 172.12, 159.65, 159.47, 147.46, 141.85, 140.98, 138.51, 137.98, 137.33, 136.78, 136.10, 135.97, 133.28, 132.02, 129.88, 129.74, 129.61, 129.50, 129.01, 128.22, 127.31, 120.03, 118.11, 116.12, 114.73, 113.65, 108.87, 106.31, 70.19, 69.61, 51.96, 43.04, 42.96, 39.01, 33.87, 33.05, 29.70, 29.42, 29.34, 28.80, 28.71, 28.66, 25.33; HRMS (ESI^+): *m*/*z* = 901.2903 $[M+NH_4]^+$ (calcd. 901.2904 for $C_{45}H_{53}N_6O_6S_4$).

Note: Assignment of the ^{1}H NMR signals was accomplished by means of 2-D NMR (COSY, ROESY, HMQC, HMBC).

2. Optimization and Reproducibility of Exchange Processes

Finding conditions that reliably, efficiently and in a practical period of time lead to equilibrium between two walking isomers (e.g. *3,4* and *2,3*; see section 1 for structures) was an important achievement in our investigation of the dynamic properties of the walker-track conjugates. In model studies on a related cyclic compound, containing both an internal acyl hydrazone and a disulfide bond, we had previously identified conditions that lead to a relatively fast dynamic exchange of hydrazone or disulfide linkages, while the other is strictly inert. There were, however, two challenges that we could not address with model systems: The first was to find optimally dilute conditions for the exchange processes to occur predominantly intramolecularly. For this we varied the concentration and the amounts of all reagents over a vast range. The second challenge was to make sure that an experimentally found ratio, e.g. between the *1,2* and the *2,3* isomer, truly represented the thermodynamic minimum. The same experiment was therefore independently conducted starting from *1,2* and from *2,3*. Only when it was found that the outcome was the same in both cases, we could assume that the true equilibrium was found.

For the hydrazone exchange (e.g. between *1,2* and *2,3* isomer) we found that adding trifluoroacetic acid (TFA) to a 0.1 mM solution of the walker-track conjugate in chloroform ($CHCl_3$) led to reliable, extremely efficient (essentially quantitative; no detectable amounts of oligomers or other side products) conversion towards the thermodynamic minimum. Since the $CHCl_3$ we used contained varying amounts of water, which is (catalytically) required in the mechanism for hydrazone exchange, we found that the time until equilibrium is reached can vary from 3 hours to over one week when only TFA is used. Such an enormous fluctuation can be avoided when a stock solution containing 20% TFA and 1% water in $CHCl_3$ is used to initiate the equilibration. For the reversible disulfide exchange we found that optimal conditions involved 0.1 mM concentration in $CHCl_3$, the strong base 1,8-diazabicyclo[5.4.0]undec-7-ene (DBU), the mild reducing agent DL-dithiothreitol (DTT), and dimethyl 3,3'-disulfanediyldipropanoate ($(MeO_2CCH_2CH_2S)_2$), the placeholder disulfide. DTT promotes disulfide exchange by acting as a source of reduced thiol species, which, when deprotonated by the base, can undergo thiol-disulfide exchange. The placeholder disulfide is added to optimize the amount of monomeric products; in its absence higher amounts of oligomers are formed. This optimized procedure reliably leads to the thermodynamic minimum in yields of ~80 % (HPLC) within about 12 hours equilibration time (see experimental section in main text for the precise conditions for hydrazone and disulfide exchange).

3. HPLC Traces

Figure S1 shows the HPLC chromatograms of the mixtures that resulted from biased operation over two cycles starting from pristine *3,4*-**C$_3$** (Fig. S1a) and *3,4*-**C$_4$** (Fig. S1b). For more detailed information see figure caption, for information on the chromatographic method see section 1.1.

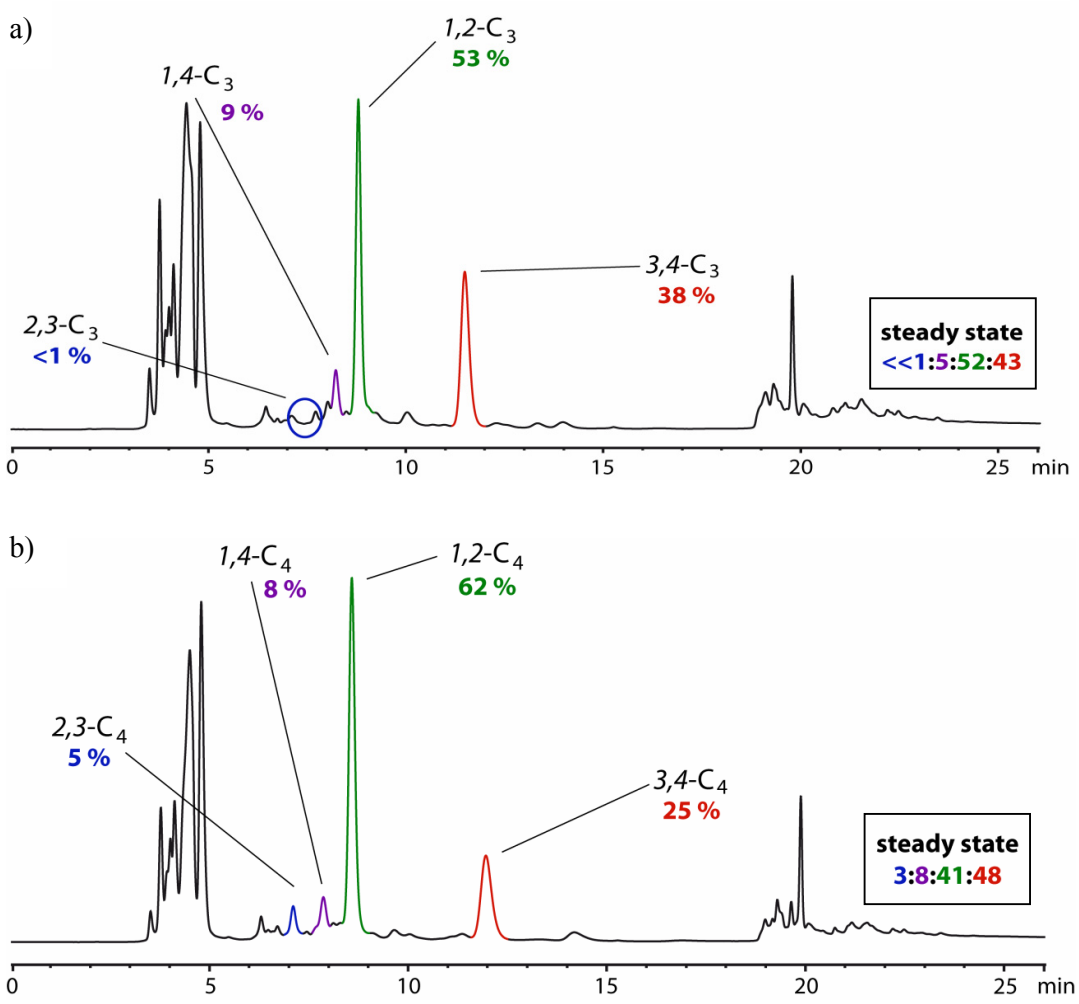

Fig. S1. Normal-phase HPLC chromatograms of the mixtures that resulted from two biased operational cycles starting from pristine *3,4*-**C$_3$** (a) and from pristine *3,4*-**C$_4$** (b). Each operational cycle involved two steps: (1) kinetically controlled disulfide exchange (condition III: (i) 1.0 mM, DTT (6 equiv.), DBU (3 equiv.), $CHCl_3$, reflux, 2-12 h; (ii) $MeO_2CCH_2CH_2SH$ (8 equiv.), I_2, Et_3N, $CHCl_3$/cyclohexane 1:1, RT, 5 min); (2) reversible hydrazone exchange (condition I: 0.1 mM, TFA, $CHCl_3$, RT, 6-96 h). The samples were not subjected to any form of purification other than simple aqueous work-up procedures. As a consequence both samples show a significant amount of unpolar impurities that were mostly brought in by solvents and reagents (analysis of UV and MS spectra provided by photo diode array (PDA) and MS detectors). The percentage values shown in this Figure are corrected for molar absorptivities (see section 4). The calculated steady state compositions (see section 6) are shown in the boxes for comparison. The identification of the isomers was greatly assisted by their unique UV spectra (PDA detector; see section 6 for UV-Vis data).

4. Processivity Study - Double-labeling crossover experiment under biased and non-biased operation

Note: The study for the non-biased mode of operation was already described previously.[1] For the benefit of clarity and to allow direct comparison, we are presenting the results for both biased and non-biased operation here.

To determine the approximate loss of processivity during non-biased and biased walking cycles, we conducted two double-labeling crossover studies based on LCMS analysis. The principle behind these studies is shown in Scheme S3. A 1:1 mixture of compounds *3,4*-**C$_5$** and *3,4*-**C$_5$**-d$_4$ was subjected to two full cycles of non-biased (conditions II and I) and biased (conditions III and I) exchange experiments. Compound *3,4*-**C$_5$**-d$_4$ differs from *3,4*-**C$_5$** by having a d$_2$-label in both the track and walker moiety. The objective was to measure the amount of d$_2$-labelled species that was formed during two full operation cycles and thus determine the level of processivity of the walking process.

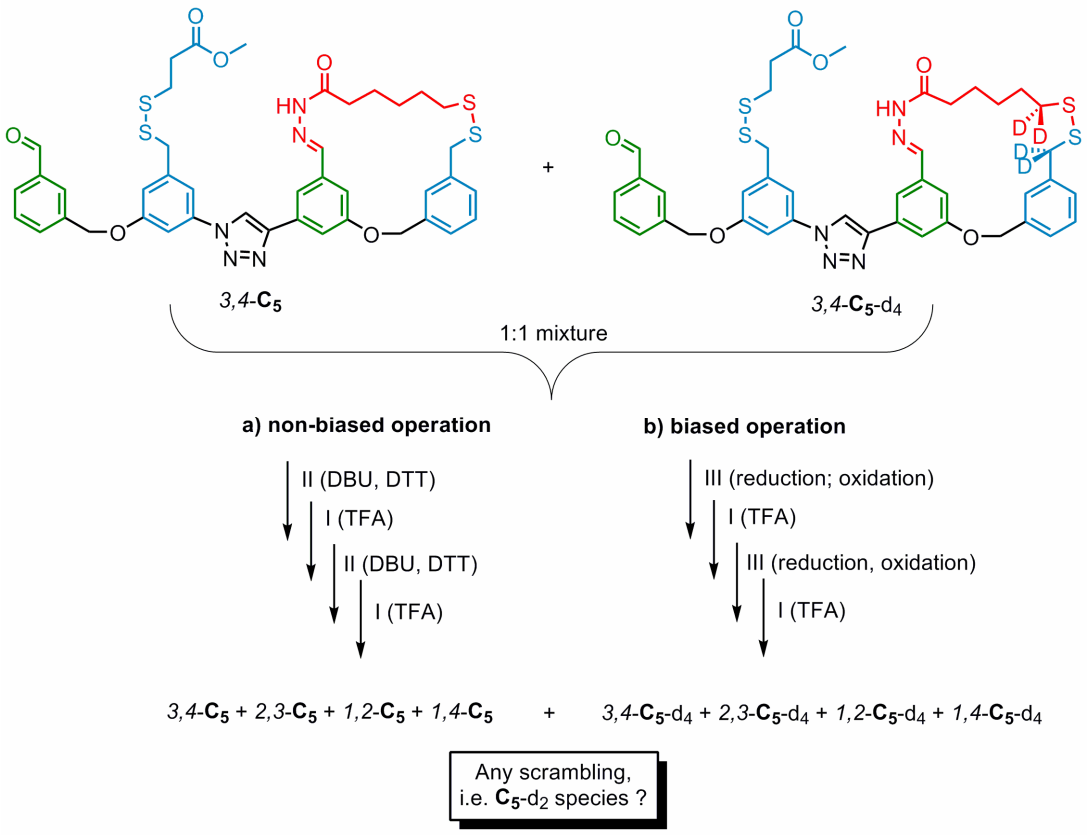

Scheme S3. Concept of the double-labeling crossover experiment. (a) non-biased, (b) biased operation.

Such d_2-labeled compounds are indicators for loss of processivity (i.e. walker no longer connected to original track), which can theoretically take place in three ways (Scheme S4). During the first pathway (a), the walker moiety completely detaches from its corresponding track and subsequently reattaches to a different track. During the second pathway (b), the loss of processivity occurs indirectly via particular types of oligomers, of which only one example, a d_0-d_4 dimer, is depicted in Scheme S4. The third pathway (c) can take place via two monomeric side products that we never detected in measurable quantities during non-biased operation, but that were observed during the kinetically controlled disulfide exchange step of the biased operation.

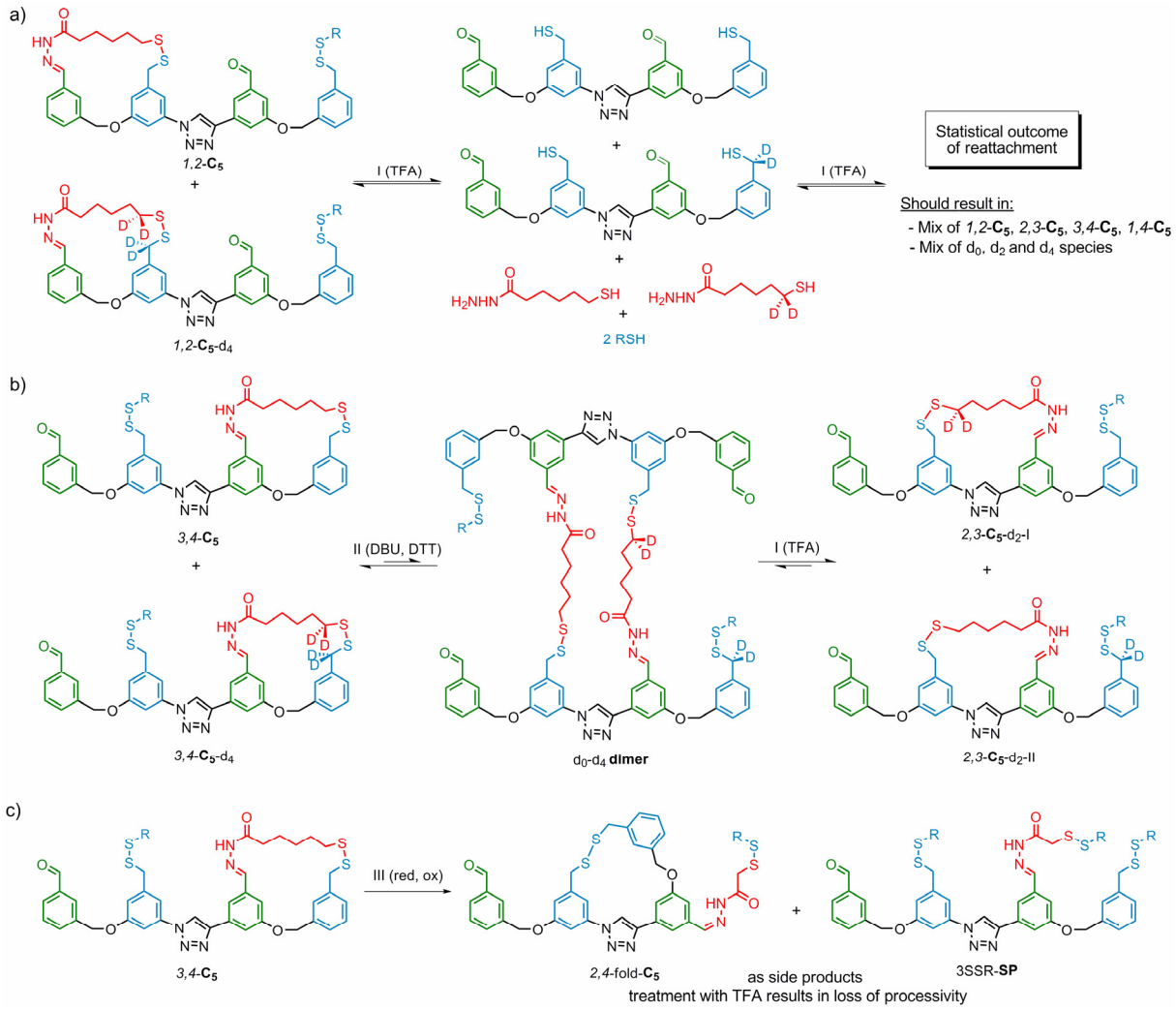

Scheme S4. Three possible pathways (a), (b), and (c) of the double-labeling crossover experiment during which d_2-species are formed and processivity is lost; a) Complete detachment of the walker moiety and statistical reattachment; b) Processivity loss via a d_0-d_4 dimer, leading to formation of d_2-species *2,3*-**C$_5$**-d_2-I, and *2,3*-**C$_5$**-d_2-II; c) Processivity loss via side products *2,4*-fold-**C$_5$** (folding of track) and 3SSR-**SP** (all three thiol vacancies occupied by placeholder thiol). Since those side products are energetically unfavorable, they were only detected under kinetic control (condition III), but not under thermodynamic control (condition II).

We are able to rule out pathway (a) for both biased and non-biased operation by means of conventional HPLC and LCMS (starting from one pristine isomer, we only found a mix of two isomers, not all four; i.e. under acidic conditions *1,2*-$\mathbf{C_5}$ only gave *2,3*-$\mathbf{C_5}$ but never *3,4*-$\mathbf{C_5}$ or *1,4*-$\mathbf{C_5}$; likewise, under basic conditions *1,2*-$\mathbf{C_5}$ only gave *1,4*-$\mathbf{C_5}$ but never *2,3*-$\mathbf{C_5}$ or *3,4*-$\mathbf{C_5}$). We can also rule out pathway (c) for the non-biased mode of operation, since we never detected side products *2,4*-fold-$\mathbf{C_5}$ and 3SSR-**SP** under reversible disulfide exchange condition II. Thus, the main objective of this experiment was to find out if, and to which extent, processivity is lost during non-biased operation (conditions II and I) via oligomer formation (pathway (b) in scheme S4) and by how much processivity loss is higher during biased operation (conditions III and I), due to side products *2,4*-fold-$\mathbf{C_5}$ and 3SSR-**SP** (pathway (c) in scheme S4).

The results of the mass spectrometric experiments and statistical and mathematical analysis are presented in the following sections. Section 3.1 shows the isotopic distribution of the 1:1 mixture of *3,4*-$\mathbf{C_5}$ and labeled *3,4*-$\mathbf{C_5}$-d_4 before any operation (serves as reference). Section 3.2 shows the isotopic distribution after two cycles of non-biased operation (conditions II and I) and section 3.3 shows the distribution after two cycles of biased operation (conditions III and I; see Scheme S3). In sections 3.4 and 3.5 the results are analyzed and discussed.

4.1. MS analysis of reference mixture of *3,4*-C_5 and *3,4*-C_5-d_4 (1:1) before operation

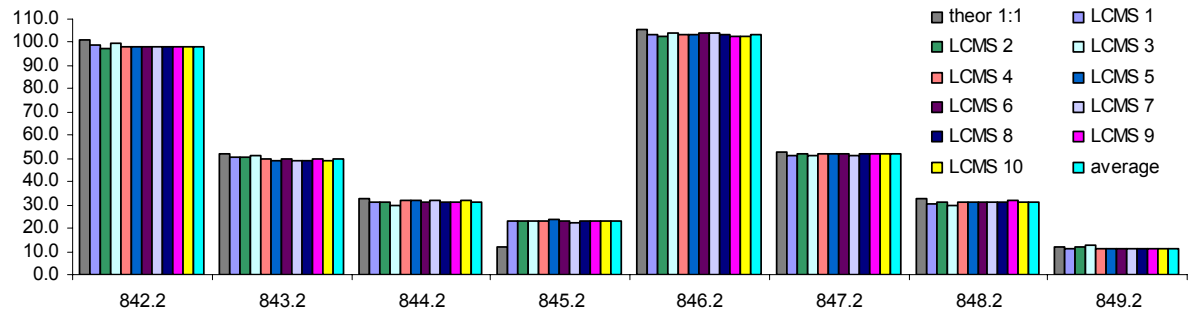

Fig. S2. Chart of theoretical, found and average isotopic distributions for the reference mixture of *3,4*- **C_5** and *3,4*- **C_5**-d_4 (1:1) before operation. For each of the ten measurements the sum over all 8 abundances (m/z 842.2 to m/z 849.2) was normalized to a value of 400.

m/z	Theor	LCMS 1	LCMS 2	LCMS 3	LCMS 4	LCMS 5	LCMS 6	LCMS 7	LCMS 8	LCMS 9	LCMS 10	Mean	Stddev.
842.2	101.1	98.6	97.5	99.6	98.3	97.8	98.2	98.4	98.3	98.1	98.4	98.3	0.5
843.2	51.8	50.4	50.3	51.0	49.7	48.7	49.4	49.2	49.4	50.2	49.4	49.8	0.7
844.2	**32.5**	**31.4**	**31.3**	**29.6**	**31.9**	**32.3**	**31.0**	**31.8**	**31.6**	**31.4**	**31.9**	**31.4**	**0.7**
845.2	11.9	23.4	23.4	22.9	22.9	23.7	22.9	22.6	23.1	23.0	22.8	23.1	0.3
846.2	105.3	103.5	102.4	103.7	102.9	103.0	104.3	104.3	103.2	102.5	102.8	103.3	0.7
847.2	53.0	51.1	52.1	51.0	52.1	51.9	51.9	51.2	52.3	52.2	51.9	51.8	0.5
848.2	32.4	30.5	31.3	29.8	31.1	31.3	31.0	31.2	31.1	31.6	31.5	31.0	0.5
849.2	11.9	11.1	11.7	12.3	11.1	11.2	11.2	11.3	11.1	11.0	11.3	11.3	0.4

Table S1. Isotopic distributions of reference mixture and statistical analysis. Theor: theoretical isotopic distribution; Mean: average of LCMS 1 to 10; Stddev.: standard deviation. The theoretical isotopic distribution was calculated as a 1:1 sum of the expected individual distributions for the d_0- and the d_4-labeled compounds. As a result of the normalization, which is necessary for the comparison of the results before and after operation, the sum of columns 2 to 12 is 400.

4.2. MS analysis of mixture of *3,4*-C_5 and *3,4*-C_5-d_4 (1:1) after operation over two non-biased cycles

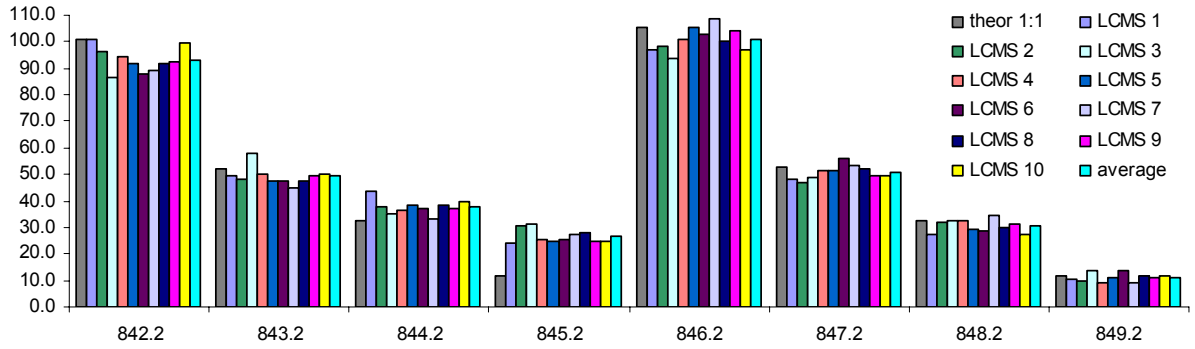

Fig. S3. Chart of theoretical, found, and average isotopic distributions of the operated mixture of *3,4*-C_5 and *3,4*-C_5-d_4 (1:1) after non-biased operation (conditions I and II). For each of the ten measurements the sum over all 8 abundances (m/z 842.2 to m/z 849.2) was normalized to a value of 400.

m/z	Theor	LCMS 1	LCMS 2	LCMS 3	LCMS 4	LCMS 5	LCMS 6	LCMS 7	LCMS 8	LCMS 9	LCMS 10	Mean	Stddev.
842.2	101.1	101.0	96.5	86.8	94.4	92.1	88.1	89.0	91.6	92.7	99.4	93.2	4.7
843.2	51.8	49.4	48.3	58.1	50.1	47.8	47.4	45.2	47.2	49.6	50.4	49.3	3.5
844.2	**32.5**	**43.4**	**37.7**	**35.5**	**36.2**	**38.5**	**37.3**	**33.4**	**38.3**	**37.1**	**39.6**	**37.7**	**2.7**
845.2	11.9	24.1	30.4	30.9	25.4	24.7	25.2	27.3	28.3	24.6	24.9	26.6	2.5
846.2	105.3	96.9	98.5	93.6	101.0	105.6	102.9	108.7	100.5	104.1	96.7	100.9	4.6
847.2	53.0	47.9	46.9	48.7	51.6	51.3	56.2	53.1	52.2	49.6	49.7	50.7	2.7
848.2	32.4	27.1	31.7	32.8	32.4	29.3	28.9	34.4	30.1	31.4	27.5	30.6	2.4
849.2	11.9	10.2	9.9	13.6	8.9	10.8	13.8	9.0	11.8	11.1	11.8	11.1	1.7

Table S2. Isotopic distributions for operated mixture (non-biased) and statistical analysis. Theor: theoretical isotopic distribution; Mean: average of LCMS 1 to 10; Stddev.: standard deviation. The theoretical isotopic distribution was calculated as a 1:1 sum of the expected individual distributions for the d_0- and the d_4-labeled compounds (assuming no processivity loss). As a result of the normalization, which is necessary for the comparison of the results before and after operation, the sum of columns 2 to 12 is 400.

4.3. MS analysis of mixture of *3,4*-C_5 and *3,4*-C_5-d_4 (1:1) after operation over two <u>biased</u> cycles

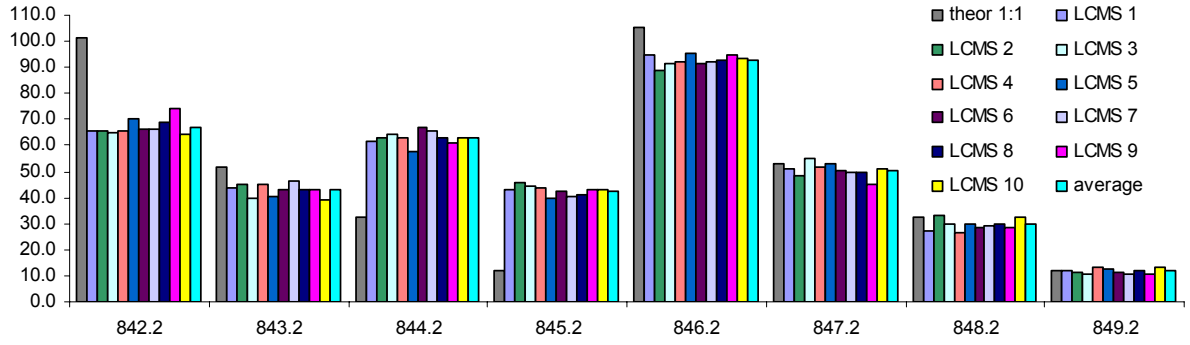

Fig. S4. Chart of theoretical, found, and average isotopic distributions of the operated mixture (biased) of *3,4*-C_5 and *3,4*-C_5-d_4 (1:1) after biased operation (conditions I and III). For each of the ten measurements the sum over all 8 abundances (m/z 842.2 to m/z 849.2) was normalized to a value of 400.

m/z	Theor	LCMS 1	LCMS 2	LCMS 3	LCMS 4	LCMS 5	LCMS 6	LCMS 7	LCMS 8	LCMS 9	LCMS 10	Mean	Stddev.
842.2	101.1	65.7	65.7	64.7	65.6	69.9	65.9	66.2	68.9	74.2	64.3	67.1	3.0
843.2	51.8	44.0	44.9	39.5	44.7	40.7	43.1	46.6	43.4	43.0	39.1	42.9	2.4
844.2	32.5	61.9	63.1	64.1	62.7	57.9	67.2	65.3	62.7	60.8	63.1	**62.9**	2.5
845.2	11.9	42.7	45.5	44.5	43.6	39.5	42.5	40.7	41.0	43.3	43.3	42.7	1.8
846.2	105.3	95.1	88.7	91.5	91.8	95.7	91.2	92.0	92.7	95.1	93.8	92.7	2.2
847.2	53.0	51.0	48.4	54.8	51.7	53.3	50.5	49.9	49.6	44.9	51.1	50.5	2.7
848.2	32.4	27.4	32.8	29.9	26.7	30.1	28.4	29.1	30.0	28.4	32.5	29.5	2.0
849.2	11.9	12.1	10.9	10.9	13.1	12.9	11.1	10.4	11.9	10.3	12.9	11.6	1.1

Table S3. Isotopic distributions for operated mixture (biased) and statistical analysis. Theor: theoretical isotopic distribution; Mean: average of LCMS 1 to 10; Stddev.: standard deviation. The theoretical isotopic distribution was calculated as a 1:1 sum of the expected individual distributions for the d_0- and the d_4-labeled compounds (assuming no loss of processivity). As a result of the normalization, which is necessary for the comparison of the results before and after operation, the sum of columns 2 to 12 is 400.

4.4. Interpretation of the MS data for non-biased operation

To assess the degree of processivity loss, we needed to quantitatively compare the average isotopic distributions that were obtained before (section 3.1, Fig. S2 and Table S1) and after (section 3.2, Fig. S3 and Table S2) operation. Fig. S5 shows a direct comparison of the experimentally obtained average distributions before (grey) and after (blue) operation. It was shown in Scheme S3 and S4 that loss of processivity would result in formation of d_2-labeled species, which have the highest isotopic abundance at m/z 844.2. When comparing the grey and blue bar at m/z 844.2 it becomes clear that after operation, m/z 844.2 shows a significant increase (by x = 6.3, Fig. S5). Fig. S5 furthermore shows the isotopic distribution that would be expected if complete statistical scrambling occurred (yellow bars). It was calculated as a 1:2:1 sum of the isotopic distributions of *3,4*-$\mathbf{C_5}$, *3,4*-$\mathbf{C_5}$-d_2 and *3,4*-$\mathbf{C_5}$-d_4 and was, in the same way as the other two data series, normalized to 400.

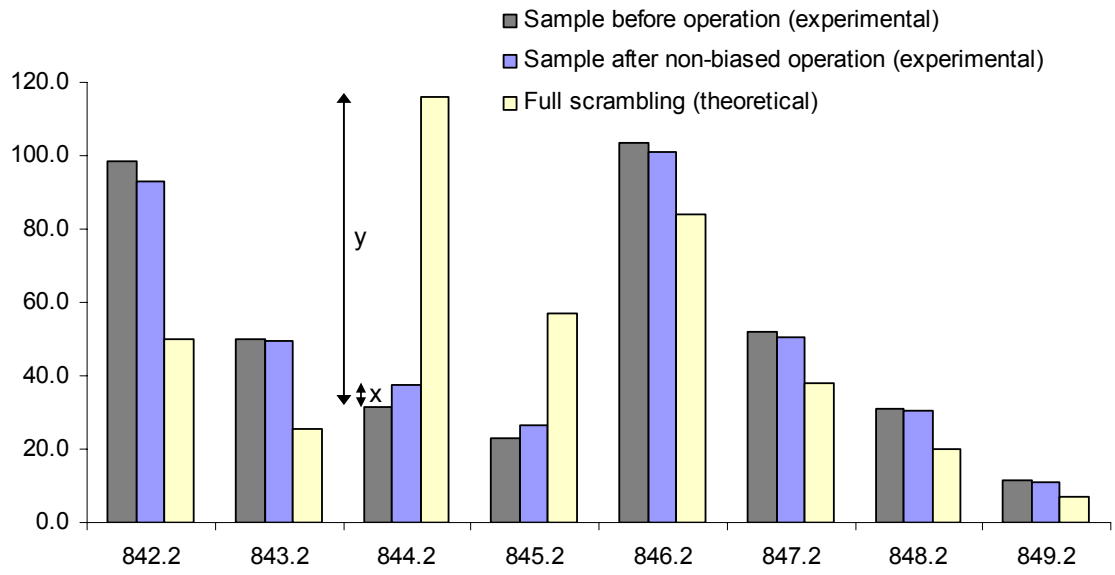

Fig. S5. Chart of mean observed isotopic distribution of sample before operation (grey) and sample after non-biased operation (blue), compared to theoretical distribution for full statistical scrambling (yellow). For all three data series the sum over all 8 abundances (m/z 842.2 to m/z 849.2) was normalized to a value of 400.

We will now consider two extreme cases in order to explain our calculation of the degree of processivity loss. In the first case the blue bar (after operation) would have the exact same height as the grey bar (before) and we would conclude that the loss of processivity is 0 %; in all molecules the walker moieties would still be connected to the same track. In the other extreme we would find that the blue bar is equal in height to the yellow bar, from which we would conclude that processivity loss is 100 %, full statistical scrambling would

have occurred. To assess results that lie in between these extreme cases we simply have to divide difference value "x" by difference value "y" (shown in Fig. S5), which gives the fraction of molecules in which the walker moiety is no longer connected to the original track. Table S4, which sums up the key conclusions from this study, shows that this value is 7.4 %. Since this relative loss of processivity in our experiment has occurred over four steps, division by four gives an average loss of processivity during one operational step of 1.9 %.

m/z	**Before operation** (experim.)	**After operation** (experim.)	**Full scrambling** (theoretical)	**Processivity loss in %** (x/y)	**Processivity loss during 1 step (in %)**	**Function for processivity decay** (p; n = steps)	**Mean step number**
844.2	31.4	37.7	116.0	7.4	1.9	$p = p_0^{(1-0.019)n} = p_0^{0.981n}$	37

Table S4. Summary of the key deductions drawn from the experimental data. The first three values can be read from Fig. S5 and Tables S1 and S2, respectively. The processivity loss of 7.4 % was calculated as x/y*100, with x = 37.7-31.4 and y = 116.0-31.4. Note that this procedure is only accurate due to the normalization of all three isotopic distributions. The processivity loss during one step results from division of 7.4 % by 4. The exponential function for processivity decay describes the level of processivity in the system p after n steps, where p_0 is the level of processivity to start with (typically: p_0=1). The mean step number is calculated from the exponential function by equation (ii) in Fig. S6 and gives the number of steps after which in 50 % of the molecules the walker moiety is no longer connected to the original track.

The level of processivity of the system, or in other words the fraction of molecules in which the walker moiety is still connected to its original track, can now be described by an exponential function (equation and graph shown in Fig. S6). The exponential decay gives a mean step number of 37 at which a molecule loses its processivity, which corresponds to an average run length along a hypothetical infinite track of approximately 26 nm. This average run length was calculated by multiplication of the mean step number with half the length of the repeat unit of our molecular track (1.4 nm). The length of the repeat unit was determined by means of molecular modeling at the B3LYP/cc-pVDZ level of density functional theory.[5]

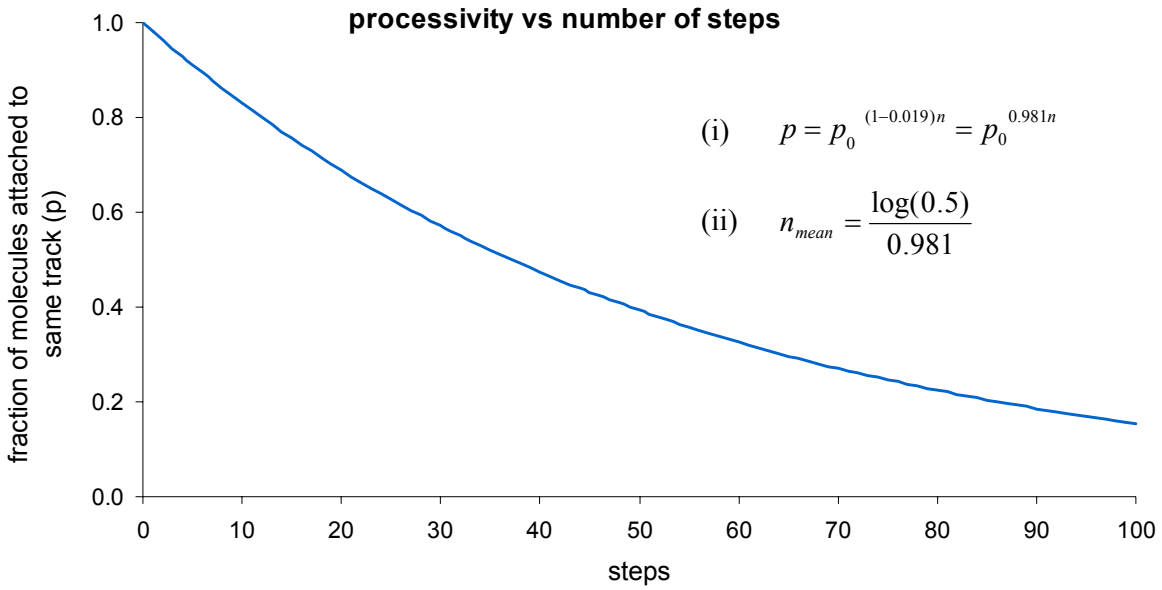

Fig. S6. Decay of processivity as described by the exponential function (i). p = fraction of molecules attached to same track; p_0 = initial fraction of molecules connected to original track (in the graph p_0 = 1.0); n = number of steps. Mean step number n_{mean} was calculated according to equation (ii).

4.5. Interpretation of the MS data for <u>biased</u> operation

The data obtained after two biased experimental cycles (presented in section 3.3) was analyzed in the same way as outlined above for the non-biased experiment. Table S5 and Fig. S7 show the results.

m/z	**Before operation** (experim.)	**After operation** (experim.)	**Full scrambling** (theoretical)	**Processivity loss in %** (x/y)	**Processivity loss during 1 step (in %)**	**Function for processivity decay** (p; n = steps)	**Mean step number**
844.2	31.4	62.9	116.0	37.2	9.3	$p = p_0^{(1-0.093)n} = p_0^{0.907n}$	7

Table S5. Summary of the key deductions drawn from the experimental data. The first three values can be read from Fig. S5 and Tables S1 and S3 respectively. The processivity loss in % was calculated as x/y*100, with x = 62.9-31.4 and y = 116.0-31.4. Note that this procedure is only accurate due to the normalization of all three isotopic distributions. The processivity loss during one step results from division of the previous value by 4. The exponential function for processivity decay describes the level of processivity in the system p after n steps, where p_0 is the level of processivity to start with (typically: p_0=1). The mean step number is calculated from the exponential function (in column 7) and gives the number of steps after which in 50 % of the molecules the walker moiety is no longer connected to the original track.

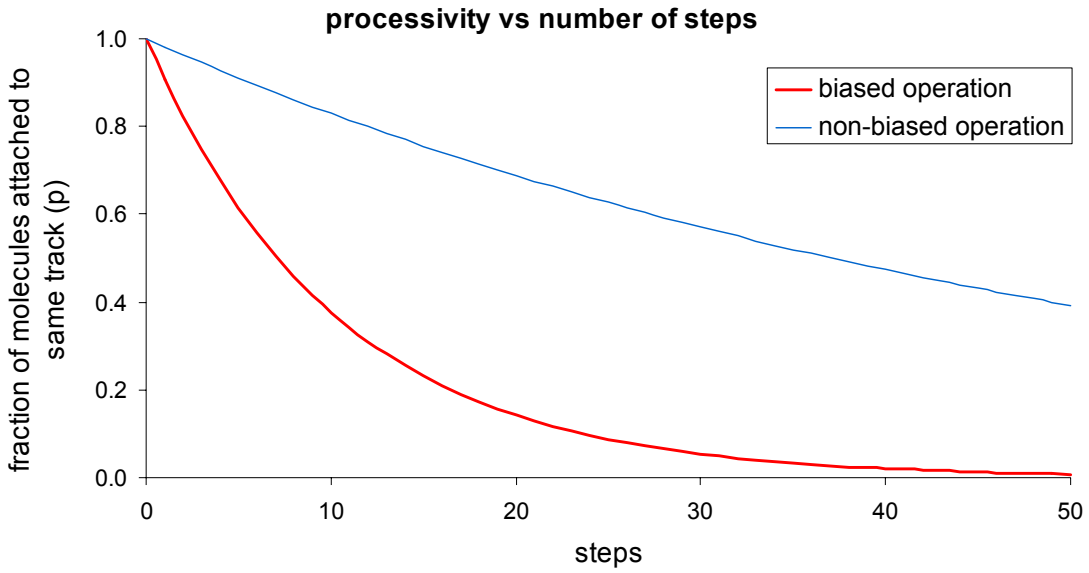

Fig. S7. Processivity vs. number of steps during non-biased (blue line) and biased operation (red line).

From Fig. S7 it becomes clear that the two modes of operation differ significantly in their degree of processivity. While the mean step number for non-biased operation is 37, the mean step number for biased operation is 7. This means that after 7 steps half of the walker moieties are no longer connected to their original track.

We can explain this rather high loss of processivity during biased operation by the higher amount of side products and oligomers that are occurring when the disulfide exchange reactions are carried out under kinetic, instead of under thermodynamic control. Side products (pathway c) and oligomers (pathway b) can lead to d_2-labeled products in the subsequent TFA catalyzed step. Indeed, we have found that after the first operational step (conditions II or III) no d_2 species were formed under both biased and non-biased conditions. It was only after the second operational step (condition I: TFA) that we detected a small increase of d_2-species in the non-biased experiment and a more pronounced increase in the biased experiment.

5. Molar Absorptivities ε and UV-Vis Data of All Studied Isomers

The molar absorptivities of compounds *1,2*-**C$_5$**, *2,3*-**C$_5$**, *3,4*-**C$_5$**, and *1,4*-**C$_5$** have been determined as previously described[1]. Table S6 shows the obtained ε values.

Isomer	Relative ε	Absolute ε (10^3 cm^2mol^{-1})
2,3-**C$_5$**	1.08	16300
1,4-**C$_5$**	1.29	19500
1,2-**C$_5$**	1.24	18700
3,4-**C$_5$**	1.00	15100

Table S6. Relative and absolute molar absorptivities ε of positional isomers *1,2*-**C$_5$**, *2,3*-**C$_5$**, *3,4*-**C$_5$**, and *1,4*-**C$_5$**. Wavelength: 290 nm; solvent: CH_2Cl_2; estimated error margin: 2-5%.

The set of relative molar absorptivities (second column in table S6) was used to calculate molar isomer ratios from the integration of HPLC traces (UV detection at 290 nm).

In theory, it would have been possible to apply the same approach to the isomers of the compound series **C$_2$**, **C$_3$**, **C$_4$** and **C$_8$**. In practice, however, this would have been very difficult to achieve and would have led to ε values with a much higher experimental error than 5 %. The first reason for this is that for **C$_2$**, **C$_3$**, **C$_4$**, and **C$_8$** only the *3,4* isomer has been synthesized (for **C$_5$** the *1,2* isomer was prepared as well). As a consequence isomers *2,3*, *1,4* and *1,2* would have had to be prepared by "walking" experiments (the *1,2* isomer even in two steps) and subsequent isolation by preparative HPLC. The second reason is that, only a very small quantity of isomers *2,3*-**C$_3$** and *2,3*-**C$_4$** would have been accessible, due to the presence of significant ring strain.

We thus decided to use the set of relative molar absorptivities that we determined for **C$_5$** (Table S6) for **C$_3$**, **C$_4$** and **C$_8$** as well (no ε values were required for the discussion of the results of **C$_2$**), since the UV spectra of the positional isomers appear to be largely independent of the length of the spacer chain in the walker moiety (spectra recorded with diode array detector; spectral comparison of corresponding compounds generally gave >99% similarity[6]). To illustrate this, Figures S8-S10 show a superimposition of the UV spectra of *3,4*-**C$_3$**, 3,*4*-**C$_4$** and *3,4*-**C$_8$** each with *3,4*-**C$_5$**.

We are aware that, particularly for the most strained **C$_3$** system, there is a certain difference in the spectra, which will have an impact on the relative ratios given in this paper. We are taking this into account, however, by giving a rather conservative ± 3 % error margin for the isomeric ratios (as compared to ± 2% for **C$_5$**). Furthermore we would like to add that, if this approach was seriously flawed, the data for the evolution of

the isomeric mixtures would necessarily be inconsistent, which is not the case. Furthermore, the main conclusions that we draw in the main text of this article could as well be drawn from non-ε-corrected HPLC data.

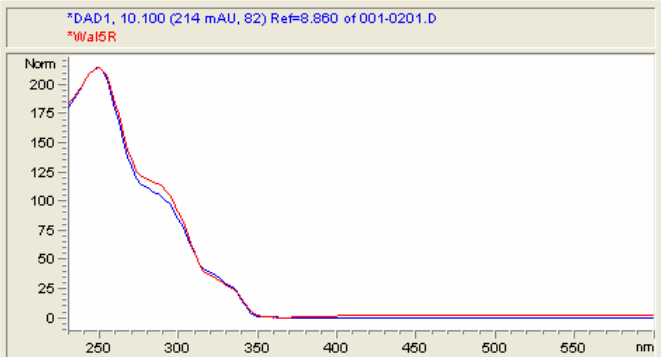

Fig. S8. Superimposition of the UV spectra of *3,4*-$\mathbf{C_5}$ (red) and *3,4*-$\mathbf{C_3}$ (blue).

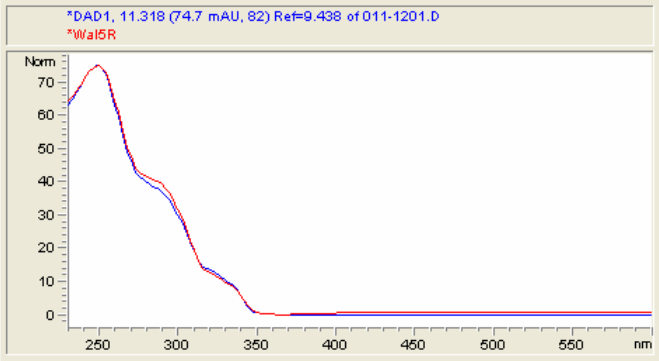

Fig. S9. Superimposition of the UV spectra of *3,4*-$\mathbf{C_5}$ (red) and *3,4*-$\mathbf{C_4}$ (blue).

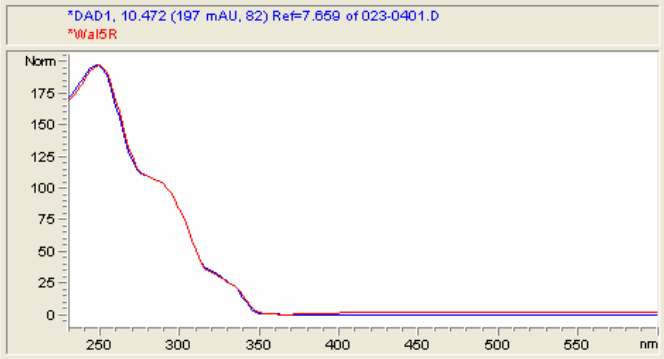

Fig. S10. Superimposition of the UV spectra of *3,4*-$\mathbf{C_5}$ (red) and *3,4*-$\mathbf{C_8}$ (blue).

Table S7 gives the local minima and maxima found in the electronic spectra of all studied isomers (*1,2*-**C$_n$**, *2,3*-**C$_n$**, *3,4*-**C$_n$** and *1,4*-**C$_n$**). The extreme similarity between positional isomers of different compound series (e.g. all compounds *1,2*-**C$_n$** have essentially identical local minima and maxima), justifies our experimental approach (characterization of each studied isomer not by NMR, for which large amounts would have been necessary, but instead by HPLC, LCMS and UV-Vis).

	1,2-**C$_n$**		*2,3*-**C$_n$**		*3,4*-**C$_n$**		*1,4*-**C$_n$**	
	local minima (nm)	local maxima (nm)	local minima (nm)	local maxima (nm)	local minima (nm)	local maxima (nm)	local minima (nm)	local maxima (nm)
C$_3$ (n=3)	264	276	278	250, 286	-	250	262	278
C$_4$ (n=4)	262	278	278	248, 286	-	250	264	276
C$_5$ (n=5)	262	278	276	248, 286	-	250	262	276
C$_8$ (n=8)	262	276	276	248, 286	-	248	262	276

Table S7. Observed local minima and maxima in the electronic spectra (recorded range: 230 nm-600 nm; solvent: CH_2Cl_2) of compound series *1,2*-**C$_n$**, *2,3*-**C$_n$**, *3,4*-**C$_n$** and *1,4*-**C$_n$**, demonstrating the similarities between positional isomers that differ only in the length of the methylene spacer (i.e. in the number n). Data obtained by photodiode array detector of HPLC instrument (see general experimental information).

6. Extrapolation of Results for C_3 and C_4 System

6.1. C_3 extrapolation

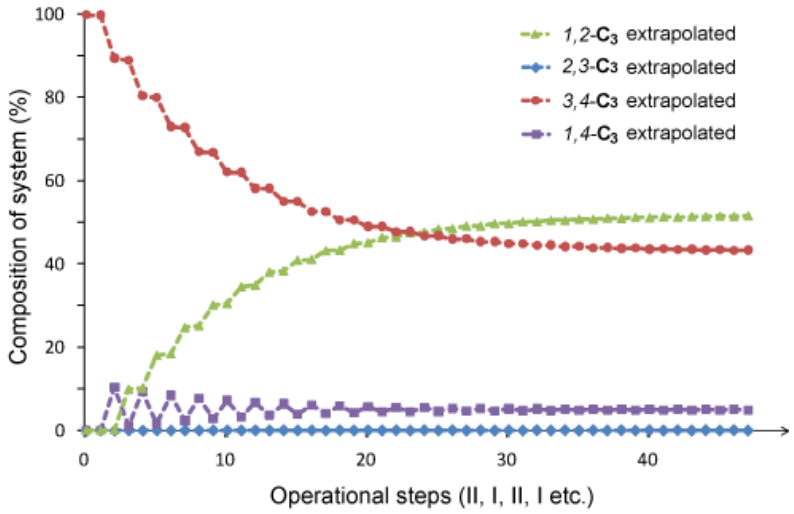

Fig. S11. Calculated composition of the $\mathbf{C_3}$ system vs. number of steps. Non-biased operation starting from 100% *3,4*-$\mathbf{C_3}$ by oscillation of conditions II and I. Calculation is based on the ratios that were determined by HPLC for the equilibria between two individual isomers. In particular, those equilibrium ratios were: *3,4*-$\mathbf{C_3}$/*1,4*-$\mathbf{C_3}$ = 90:10; *3,4*-$\mathbf{C_3}$/*2,3*-$\mathbf{C_3}$ = ~99:1; 1,*4*-$\mathbf{C_3}$/*1,2*-$\mathbf{C_3}$ = 9:91; *2,3*-$\mathbf{C_3}$/*1,2*-$\mathbf{C_3}$ = ~1:99 (results were reproducible within ± 2 %; estimated error margin due to unconventional ε correction: ± 3 %).

Conclusions: The relatively high ground state energy of *2,3*-$\mathbf{C_3}$ has two consequences: (i) when in equilibrium with another isomer (*1,2*-$\mathbf{C_3}$ or *3,4*-$\mathbf{C_3}$), the HPLC peaks belonging to *2,3*-$\mathbf{C_3}$ were very close to the (lower) detection limit, implying that for this calculation we had to make the rough assumption that 1% of *2,3*-$\mathbf{C_3}$ is present. (ii) The convergence towards the thermodynamic minimum requires a large amount of operational steps (approx. 40).

The fact that the four experimentally determined ratios between the positional isomers (see caption Fig. S11) led to convergence of the theoretical data towards a stable steady state, strongly indicates that they form a consistent set that accurately represents the relative energies of the four isomers. If, for example, in one of our extrapolation calculations, we randomly changed one of the four ratios, the graphs did no longer converge, but fluctuate. As a consequence, these calculations serve two purposes: (i) they verify the accuracy of the experimentally obtained ratios, as well as the quality of the ε correction and (ii) they allow calculation of the steady state composition, which, in the case of the $\mathbf{C_3}$ and $\mathbf{C_4}$ system, would require 30 and 15 steps, respectively, and which would therefore be too laborious to establish experimentally.

6.2. C_4 extrapolation

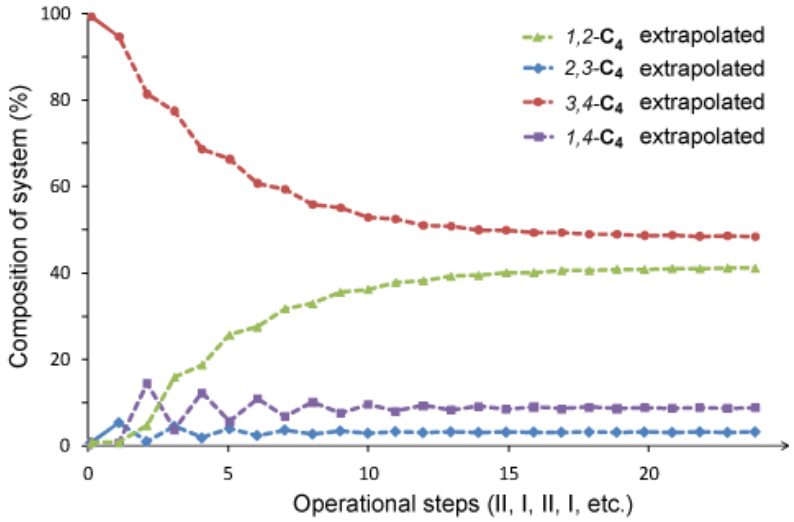

Fig. S12. Calculated composition of the C_4 system vs. number of steps. Non-biased operation starting from 100% *3,4*-C_4 by oscillation of conditions II and I. Calculation is based on the ratios that were determined by HPLC for the equilibria between two individual isomers. In particular, those equilibrium ratios were: *3,4*-C_4/*1,4*-C_4 = 85:15; *3,4*-C_4/*2,3*-C_4 = 95:5; *1,4*-C_4/*1,2*-C_4 = 16:84; *2,3*-C_4/*1,2*-C_4 = 6:94 (results were reproducible within ± 2 %; estimated error margin due to unconventional ε correction: ± 3 %).

Conclusions: Alike the C_3 system, convergence of the C_4 system towards the thermodynamic minimum requires a rather large amount of operational steps (approx. 15). The convergence indicates that the experimental data are reliable (on the same grounds as given for the C_3 system in section 5.3).

6.3. C_8 extrapolation

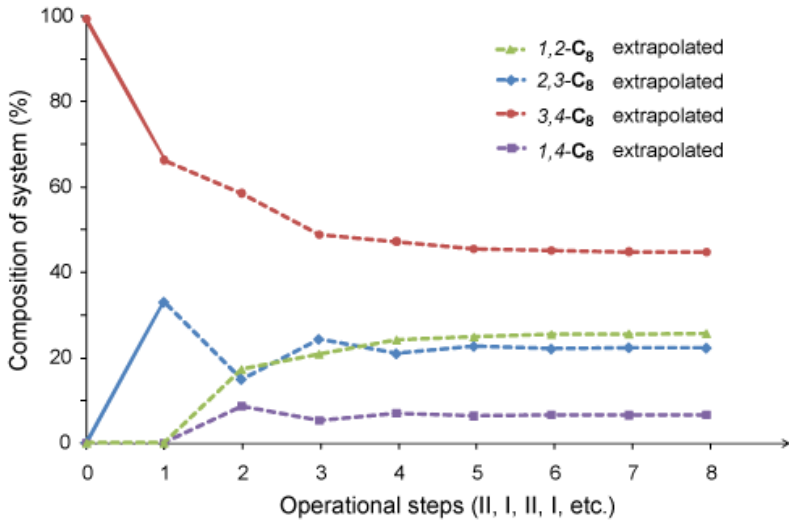

Fig. S13. Calculated composition of the **C_8** system vs. number of steps. Non-biased operation starting from 100% *3,4*-**C_8** by oscillation of conditions II and I. Calculation is based on the ratios that were determined by HPLC for the equilibria between two individual isomers. In particular, those equilibrium ratios were: *3,4*-**C_8**/*1,4*-**C_8** = 87:13; *3,4*-**C_8**/*2,3*-**C_8** = 67:33; *1,4*-**C_8**/*1,2*-**C_8** = 20:80; *2,3*-**C_8**/*1,2*-**C_8** = 46:54 (results were reproducible within ± 2 %; estimated error margin due to unconventional ε correction: ± 3 %).

Conclusions: In respect to its convergence towards the thermodynamic minimum, the **C_8** system behaves similar to **C_5**.

7. References

(1) Von Delius, M.; Geertsema, E. M.; Leigh, D. A. *Nat. Chem.* **2010**, *2*, 96-101.

(2) Costioli, M. D.; Berdat, D.; Freitag, R.; André, X.; Müller, A. H. E. *Macromol.* **2005**, *38*, 3630.

(3) Lin, D.; Zhang, J.; Sayre, L. M. *J. Org. Chem*. **2007**, 72, 9471.

(4) Klein, L. L.; Yeung, C. M.; Kurath, P.; Mao, J. C.; Fernandes, P. B.; Lartey, P. A.; Pernet, A. G. *J. Med. Chem.* **1989**, 32, 151.

(5) Gaussian 03, Revision E.01, Frisch, M. J., Trucks, G. W., Schlegel, H. B., Scuseria, G. E., Robb, M. A., Cheeseman, J. R., Montgomery, Jr., J. A., Vreven, T., Kudin, K. N., Burant, J. C., Millam, J. M., Iyengar, S. S., Tomasi, J., Barone, V., Mennucci, B., Cossi, M., Scalmani, G., Rega, N., Petersson, G. A., Nakatsuji, H., Hada, M., Ehara, M., Toyota, K., Fukuda, R., Hasegawa, J., Ishida, M., Nakajima, T., Honda, Y., Kitao, O., Nakai, H., Klene, M., Li, X., Knox, J. E., Hratchian, H. P., Cross, J. B., Bakken, V., Adamo, C., Jaramillo, J., Gomperts, R., Stratmann, R. E., Yazyev, O., Austin, A. J., Cammi, R., Pomelli, C., Ochterski, J. W., Ayala, P. Y., Morokuma, K., Voth, G. A., Salvador, P., Dannenberg, J. J., Zakrzewski, V. G., Dapprich, S., Daniels, A. D., Strain, M. C., Farkas, O., Malick, D. K., Rabuck, A. D., Raghavachari, K., Foresman, J. B., Ortiz, J. V., Cui, Q., Baboul, A. G., Clifford, S., Cioslowski, J., Stefanov, B. B., Liu, G., Liashenko, A., Piskorz, P., Komaromi, I., Martin, R. L., Fox, D. J., Keith, T., Al-Laham, M. A., Peng, C. Y., Nanayakkara, A., Challacombe, M., Gill, P. M. W., Johnson, B., Chen, W., Wong, M. W., Gonzalez, C. & Pople, J. A. Gaussian, Inc., Wallingford CT, 2004.

(6) ChemStation for LC 3D systems 3D, Rev. B.04.01 [481], Agilent Technologies Inc..